The Development and Walking Control of Biped Robot

Ruixiang ZHANG

(B.Eng, HIT)

A THESIS SUBMITTED

FOR THE DEGREE OF MASTER OF ENGINEERING

DEPARTMENT OF ELECTRICAL & COMPUTER ENGINEERING

NATIONAL UNIVERSITY OF SINGAPORE

2004

Acknowledgements

I would like to express my deep and sincere gratitude to my supervisors Dr. Prahlad Vadakkepat and Dr. Chew Chee Meng for their guidance, support and supervision during the course of the project.

I would also like to thank Dr. Abdullah Al Mamun, Dr. Ge Shuzhi, Sam Dr. Tan Kok Kiong for their invaluable advices and kind attentions to the project.

My appreciation also goes to Mr Chan Kit Wai and Mr. Tee WeiIn of the Mechatronics and Automation Lab for their assistance.

Contents

Acknowledgements ii

Contents iii

Summary vii

List of Figures ix

List of Tables xiii

1 Introduction 1

1.1 Background on bipedal locomotion 1

1.2 Objectives of the work 2

1.3 Biped Robot 4

1.4 Simulation Software 5

1.5 Thesis Contributions 6

1.6 Thesis Outline 6

2 Literature Review **8**

2.1 Biped Robot 8

2.2 Walking algorithm 15

3 Mechanical Design and Actuators **18**

3.1 Analysis of body structure 19

3.2 Selection of the material and actuators 20

3.3 Structural design 22

3.4 Upper body design 23

4 Sensors Integration and Control System Configuration **26**

4.1 Sensors 26

4.1.1 Force sensor 26

4.1.2 Tilt sensor 29

4.1.3 Digital compass 29

4.1.4 Video camera 30

4.1.5 IR sensor 31

4.1.6 Controller 32

4.2 Control system configuration 33

5 Trajectory Based Walking Algorithm 36

5.1 Single and double support phase 37

5.2 ZMP and ankle torque 38

5.3 Hip trajectory for single support phase 41

5.4 Swing foot trajectory for single support phase 45

5.5 Double support phase control 46

6 Simulation and Experiment 49

6.1 Simulation for flat ground 50

6.1.1 Gait generation 50

6.1.2 Simulation study 51

6.2 Simulation for climbing stairs 55

7 Evolution of the Trajectory Based Algorithm 60

7.1 Evolutionary algorithm 60

7.2 The evolution of the walking algorithm 63

8 Realized Functions and Algorithms 67

8.1 Robot Dash 67

8.2 Penalty kick and goal keep 68

8.3 Obstacle Run 69

9 Conclusion **71**

Bibliography **73**

Author's Publications **77**

Summary

In recent years, legged locomotion has been widely studied because of its adaptability to various grounds even to those rough terrains that are impossible for the powerful wheeled machines. Bipedal locomotion is a special kind of legged locomotion and it is more complicated and difficult to control. However, bipedal locomotion can be more suitable in unknown environments. More importantly, our human beings are biped creatures and our living environment is very suitable for bipedal locomotion. For the above two important reasons, the study of bipedal locomotion and the development of biped robot are meaningful, and the research results could be widely used in the future applications.

The purpose of this project is to build a biped robot platform and carry out the study of dynamic walking and artificial intelligence algorithms. Consequently, this project is composed of following two parts: 1) the design and development of a biped robot, and, 2) the study of biped walking algorithm.

Servo motors are used as the robot joints and various sensors are equipped on the robot. Two DSP boards are used as the controllers. The biped robot has been successfully developed and achieved the desired performance. It realizes complicated

actions such as walking avoiding obstacles and kicking a ball.

The bipedal locomotion is studied and a dynamic walking algorithm which adapts to various terrains is developed. The robot is able to start walking from any phase of a walking cycle. The trajectory based gait generation algorithm is simulated and applied successfully to the robot and dynamic walking is realized.

List of Figures

1.1 The humanoid 4

1.2 Simulation with Yobotics. 5

2.1 Passive Walker Developed by McGeer 9

2.2 Biped Robot Developed by Kajita 10

2.3 Honda Humanoid Robot 11

2.4 Wabian Humanoid Robot 12

2.5 Biped Robot SD-2 13

2.6 Biped robot developed by Shih 14

2.7 SpringFlamingo Developed in MIT Leg Lab 15

2.8 M2 3-D Biped Robot Developed in MIT Leg Lab 16

3.1 Kinematics arrangement of RoboSapien 21

3.2 The motor cover, original motor and modified motor 22

3.3 Mechanical design of legs 24

3.4 The foot design 24

3.5 Mechanical part of legs and feet 25

3.6 Body frame 25

3.7 Cover of upper body 25

4.1 Flexible force sensor 27

4.2 The response of force sensor 28

4.3 Tilt sensor 29

4.4 Digital compass 30

4.5 Video camera 31

4.6 Infra Red Sensor 32

4.7 Controller 34

4.8 Control system configuration 35

5.1 Walking cycle: single and double support phase 38

5.2 Biped robot model 39

5.3 Invert pendulum model to derive the ankle torque 40

5.4 Ankle torque range when the ZMP in the stable region 41

5.5 Hip and foot trajectory 41

5.6 Determine the height of hip 42

5.7 From unstable to stable region 47

6.1 Stick diagram of gaits in single support phase for walking on flat ground 49

6.2 The snap shots of simulation of biped locomotion on flat ground . . 50

6.3 ZMP trajectory along the walking direction 51

6.4 ZMP trajectory in the hip coordinate system 52

6.5 Ankle joint angle 53

6.6 Knee joint angle 54

6.7 Hip joint angle 55

6.8 The position and velocity of hip joint converge to a limit cycle: initial state A 56

6.9 The position and velocity of hip joint converge to a limit cycle: initial state B 57

6.10 The position and velocity of hip joint converge to a limit cycle: initial state C. 57

6.11 Biped robot walking on flat ground 58

6.12 Hip and foot trajectory for climbing stairs 58

6.13 Stick diagram of gaits in single support phase for climbing up stairs. . 59

6.14 The simulation snap shots of biped locomotion climbing stairs 59

7.1 Fitness changing with generation 64

7.2 ZMP before evolution 65

7.3 ZMP after evolution 65

7.4 Simulation of climbing stairs 66

8.1 Robot dash 68

8.2 Penalty kick 69

8.3 Goal keep 70

8.4 Obstacle run 70

List of Tables

3.1 Height and mass ratios of human body. 20

3.2 Height and mass ratios of RoboSapien. 20

3.3 Specifications of Actuators 23

7.1 Parameters for the evolutionary algorithm 63

7.2 Parameters of walking simulation 64

Chapter 1

Introduction

1.1 Background on bipedal locomotion

The locomotion of creatures has been studied for centuries. Different kind of creature has different locomotion closely related to its body structure. The body structure evolves with generation adaptive to the living environment. Legged locomotion has higher adaptability and is widely studied recently. Legged robots can walk in rough terrains including those that are impossible for the wheeled machines.

Compared to the other legged creatures, biped creatures are more dextrous and have higher mobility especially in complicated environments with obstacles. More importantly, human beings are bipedal. The human's living and working environment suit the biped creatures very well. For these reasons, utilizing the biped robot in the human working environment is promising especially in areas that pose great hazard for human beings and, developing biped robots and associated control algorithms are

therefore meaningful.

Walking can be easily performed by humans. But it is a very complicated problem for the biped robot to achieve natural walking like humans. Bipedal walking is a non-linear and multi-variable dynamic system. Not only the kinematics but also the dynamics should be considered in walking control. In a bipedal system, all the links are closely related to each other and are highly coupled. The dynamics of the system is also affected by the ground reaction force.

Generally, the biped walking can be classified into static walking and dynamic walking. Static walking is characterized by keeping the Center of Gravity (COG) in the support region (the convex hull of the contact points between the foot/feet and the ground). Static walking is easy to realize while the walking speed is normally very slow. Dynamic walking is more complicated and difficult to achieve compared to static walking. In dynamic walking, the COG needs not be in the support region. There are various algorithms to realize dynamic walking.

Many biped robots have been developed in recent years [1–10] and many researchers have focused on biped robot control algorithm development [1, 3, 4, 8, 11–24].

1.2 Objectives of the work

The objectives of this work are to build a humanoid platform and to realize the dynamic walking. This project is composed of two parts: the design and development of a humanoid robot, and the study of bipedal walking algorithm.

In terms of the hardware development, the work includes mechanical design, control system configuration and sensor integration. The walking performance is closely related to the body structure. In order to realize good walking performance, the humanoid robot should satisfy the following requirements:

1. The biped robot should be able to perform most walking actions of human beings.

2. In order to realize fast dynamic walking, the robot should have light weight.

Besides, the humanoid is planned to join the FIRA Robot World Cup Competition. It should be able to realize those functions required in the FIRA Robot World Cup Competition.

There are various algorithms to realize dynamic walking. A good walking algorithm makes walking stable, natural and flexible. The objective is to synthesize a walking algorithm with the following points:

1. The walking algorithm should be applicable to flat ground, rough terrain and stairs.

2. The algorithm should be able to enable the robot to start walking from any phase of a walking cycle.

The design and development of the biped robot and the dynamic walking algorithm are introduced in detail in the subsequent chapters.

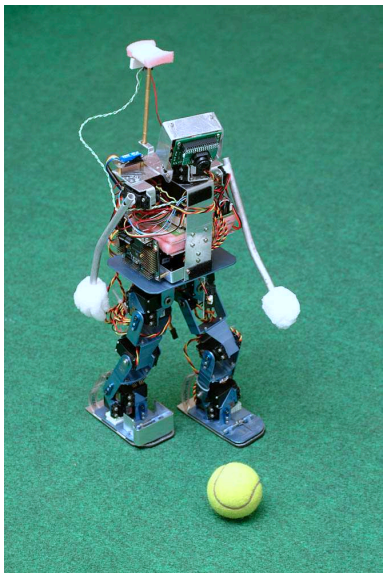

Figure 1.1: The humanoid

1.3 Biped Robot

Figure 1.1 shows the biped robot which has been designed and developed. This is a small size robot weighting 2 kg with a height of 46 cm. The robot totally has 17 degrees of freedom. It is equipped with various sensors: video camera, digital compass, Infra-red sensor, tilt sensor and force sensor. The robot is designed according to the rules of the FIRA Robot World Cup competition. The robot is able to walk fast, walk towards a direction avoiding obstacles and, locate and kick a ball. At the FIRA Robot World Cup Vienna 2003, the robot secured overall championship.

1.4 Simulation Software

Yobotics Simulation Construction Set [25], developed by the MIT Leg Laboratory, is used to simulate the walking of the biped robot.

The Yobotics Simulation Construction Set is a full-featured software package that can easily simulate robots, biomechanical systems, and mechanical devices. In this simulation software, all joint positions, velocities, and torques are accessible. It is possible to define ground contour and ground contact models. Besides, data can be recorded to plot figure and do theoretically study. Figure 1.2 shows the simulation of biped walking in Yobotics.

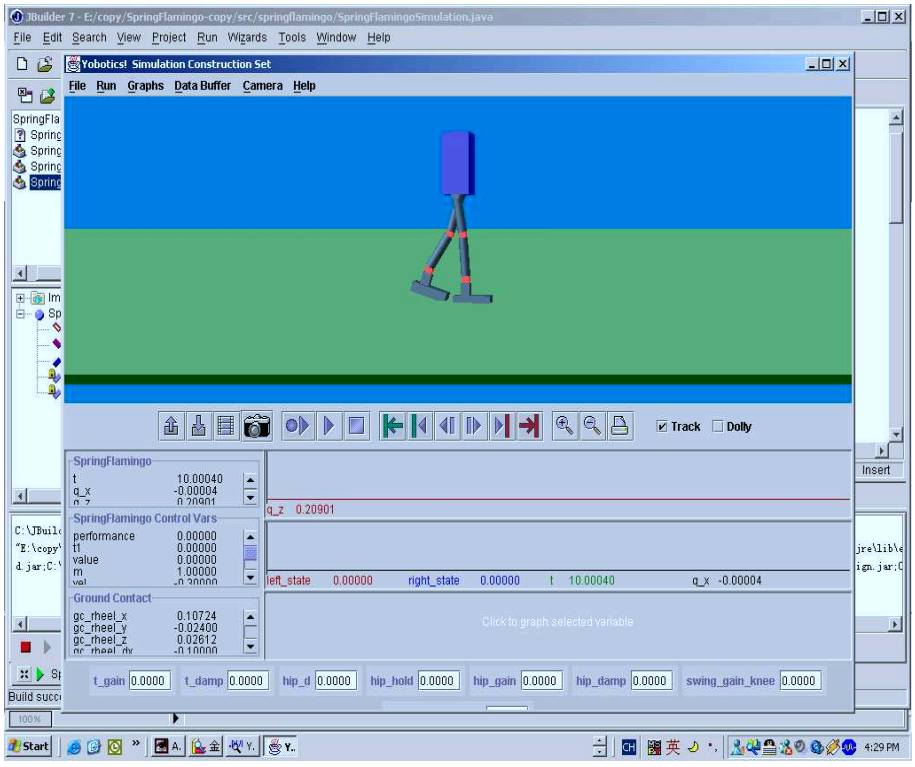

Figure 1.2: Simulation with Yobotics.

1.5 Thesis Contributions

The thesis elaborates on the robot development and walking algorithm. The contributions of the thesis are:

1. The mechanical structure design and joints arrangement of a biped robot with light weight and small size.

2. The integration and application of various sensors: force sensor, tilt sensor, video camera, Infra-red sensor and digital compass.

3. The design and development of the associated control system. Real-time control is a principal requirement in the walking control. A two-level control structure is used to realize the sensors integration, decision making and walking control.

4. The synthesis of a walking algorithm which can adapt to various terrains and that can start walking from any phase of the walking cycle.

5. The realization of the functions required in the FIRA World Cup Competition: Dash, Obstacle Run and Penalty Kick.

1.6 Thesis Outline

Chapter two provides a review of the biped robot development and walking algorithm. Dozens of biped robots have been developed in recent years. Abundant experience on building biped robot is achieved from reviewing these works.

Chapter three describes the mechanical design of the biped robot developed, including the component selection, arrangement of joints and the structural design.

Chapter four presents the sensors and the control system of the biped robot. Two DSP boards are utilized as the high level and low level controller. The communication between sensors and controllers are introduced.

Chapter five describes the dynamic walking algorithm. A trajectory based walking algorithm which can adapt to various terrains and can enable the robot to start walking from any phase of the walking cycle is synthesized.

Chapter six presents the simulation study of the synthesized walking algorithm. The simulation results show that the walking algorithm can realize walking on flat ground and climbing up stairs.

Chapter seven describes the application of evolutionary algorithm on the walking gaits evolution. The simulation results show that the performance is improved after the evolution.

Chapter eight introduces the realized functions of the humanoid, such as dash, penalty kick and obstacle run. The robot joined FIRA Robot World Cup Vienna 2003, and secured the overall championship.

Chapter nine concludes the work.

Chapter 2

Literature Review

2.1 Biped Robot

In this chapter several biped robots which had brought great influence on the study of biped walking are reviewed. Several frequently used walking algorithms are outlined.

In recent years, dozens of biped robots have been designed and developed to study and test the various biped walking algorithms.

Mc Geer [1] developed a passive dynamic walker (Figure 2.1) to study the natural passive dynamic walking. This kind of two-legged machines have natural dynamic mode of walking. Once started on a shallow slope, it settles into a steady gait quite comparable to human walking, without active control or energy input. The gait is generated by the passive interaction of gravity and inertia. The robot has only one degree of freedom. But the two legs are telescopic so that the robot can swing the leg from back to front without colliding with the ground. Only the lateral motion

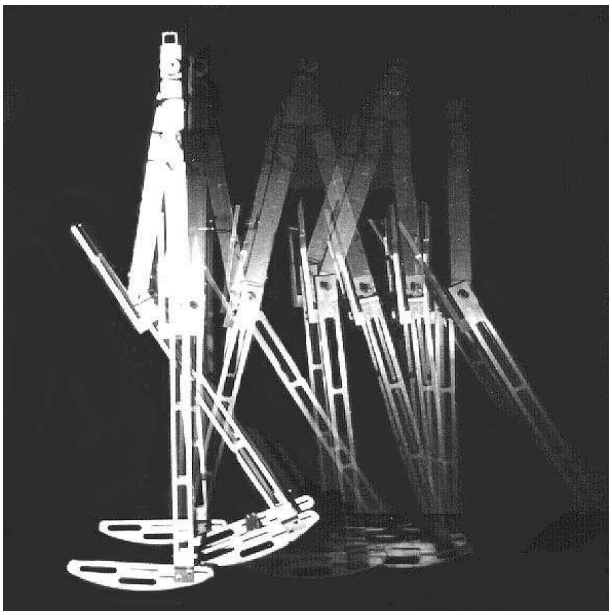

Figure 2.1: Passive Walker Developed by McGeer

is considered making it a planar robot. The idea of building a passive biped robot is inspired by a paper written by Mochon and McMahon (1980), who showed how walking could be generated by the passive interaction of gravity and inertia. The motion for studying passive walking is that it is mechanically simple and relatively efficient. McGeer has completed a simple mechanical construction and obtained a desired walking motion. The motion has been studied theoretically. The passive walker activated by gravity can only walk along a downward slope. The passive biped weights 3.5 kg and has a height of 0.5 m. It can walk at a speed of 0.46 m/s along a 2.5% downward slope.

Shuuji Kajita et al. have designed and developed a "nearly ideal" 2-D biped model with light weight legs [2] (Figure 2.2). Four DC motors are put in the body and the legs are configured as parallel link mechanisms. For simplicity, the COG of the robot

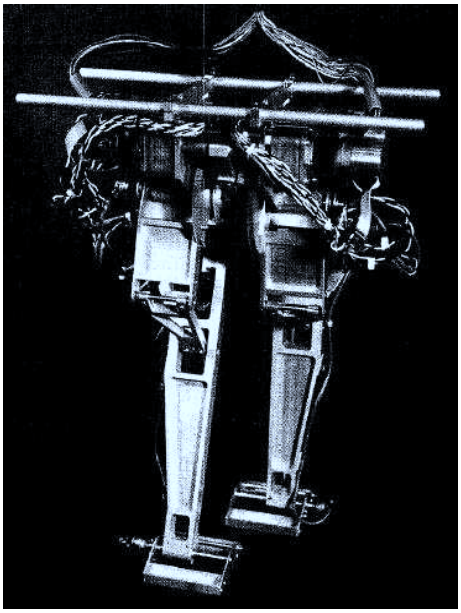

Figure 2.2: Biped Robot Developed by Kajita

is supposed to move horizontally. Control laws are formulated for walking initiation, continuation and termination. "Linear Inverted Pendulum Mode" is utilized for controlling the biped walking on rugged terrain. The six degrees of freedom biped robot developed has light-weight legs and moves in a two-dimensional vertical plane. To investigate the effects, they carried out two experiments: the support phase experiment and the support exchange experiment. The support phase experiment was carried out to check the actual dynamics of a biped walking under the proposed control. The support exchange experiment was performed to check leg support exchange. It was found that a smooth leg support exchange is achieved by making the foot contact with a certain short period. Based on these results, a whole biped control system was implemented. As reported in the experiment the robot walked over a box of 3.5 cm height at a speed of 20 cm/s.

Figure 2.3: Honda Humanoid Robot

In December 1996, Honda announced the development of a humanoid robot with two arms and two legs called P2 (Figure 2.3). Research and development of this humanoid robot was initiated in 1986. The ambitious goal was to develop a robot which is able to coexist and collaborate with humans, and even to perform tasks that humans cannot. P2 is a self-contained humanoid robot with two arms and two legs, and can be operated via wireless communication. The overall height is 1820mm, the width is 600mm, and the weight is 210kg. It has 12 degrees of freedom in two legs and its arms have 14 degrees of freedom. Each joint is actuated by a DC motor with a harmonic-drive reduction gear. Within its body is a control computer with four microprocessors running the real-time operating system VxWorks. The processors are used for the arm control, leg control, the local control of the joints, and the vision processing respectively. The body is equipped with an inclination sensor which consists of three

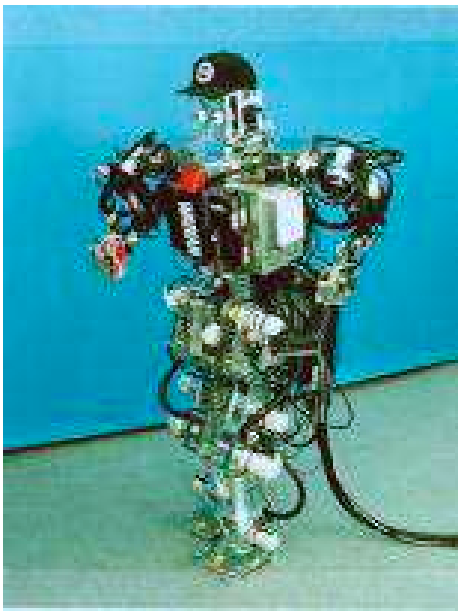

Figure 2.4: Wabian Humanoid Robot

accelerometers and three angular rate sensors. Each foot and wrist are equipped with a 6-axis force sensor. In the head of the robot, there are four video cameras. Two are used for vision processing, and the other two are used for tele-operation. P2 has been designed to maintain a stable posture by adopting human-like movements. The local controller controls the displacement of the electric motor actuators so that the robot can follow the leg joint angles of the desired walking pattern. The robot is primarily controlled by playing back pre-recorded joint trajectories acquired from direct measurements of human subjects.

Waseda University has been one of the leading research groups for anthropomorphic robots since they started the WABOT Project in 1970. Since then, just about ten years, by integrating the latest key technologies, they have developed a variety of humanoid robots including WABOT-1 which is the first full-scale human-like robot

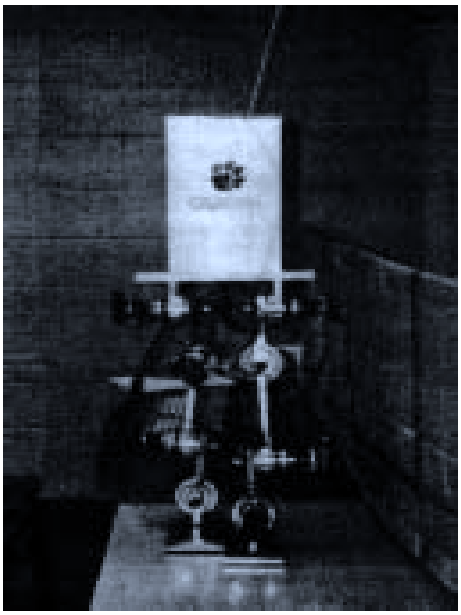

Figure 2.5: Biped Robot SD-2

made in 1973, the musician robot WABOT-2 in 1984, Hadaly-2 which works together with a human partner and the biped walking robot WABIAN in 1997 (Figure 2.4). The biped robot WABIAN has a weight of 107 kg and a height of 1.66 m. It is made of extra-super-dur-aluminum. The robot has 6 DOF on lower body, 3 DOF on the trunk, 14 DOF on the arms. The robot has 35 active DOF totally. Waseda's walking algorithms rely on playing back pre-recorded joint and trunk trajectories which produced the desired Zero Moment Point (ZMP) trajectory. The ZMP is the point on the ground around which the sum of all the moments of the active forces equals zero. In order to adapt to terrain changes or external disturbances, the desired trajectories are altered. [26]

Zheng et al. have constructed a biped robot named SD-2 [3] (Figure 2.5). A scheme to enable the robot to climb sloping surface was proposed. By means of force sensors

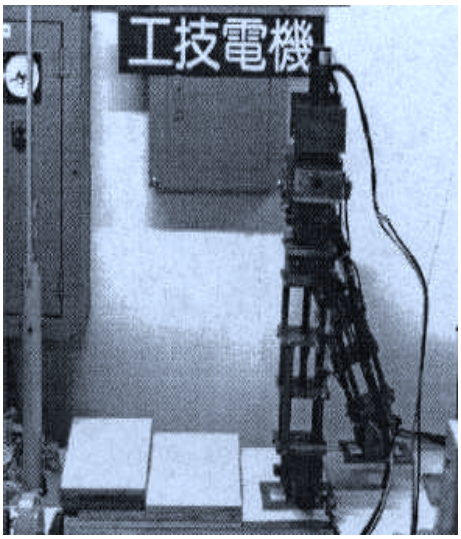

Figure 2.6: Biped robot developed by Shih

underneath the heel and toe, the robot can detect the transition of the support terrain from a flat floor to a sloping surface. The inclination of the supporting foot and slop gradient are evaluated. A compliant motion scheme is then used to shift the COG in order to achieve the transition. Miller designed a robot with knees similar to SD-2 [4].

Shih et al. have designed and developed a 7 DOF biped robot [5,11] (Figure 2.6). The robot has variable length legs and a translatable balance weight in body. Because of the latter feature, the robot is controlled easily in the lateral plane. The variable length legs enable the robot to adapt to uneven terrain easily and make the swing phase control simpler.

Springflamingo is a planar biped robot with six degrees of freedom developed at the MIT Leg Laboratory (Figure 2.7). M2 is a 3D biped walking robot (Figure 2.8) which is currently being developed in the MIT Leg Laboratory. The robot has 12 active degrees of freedom: 3 in each hip, 1 in each knee, and 2 in each ankle. It will be used

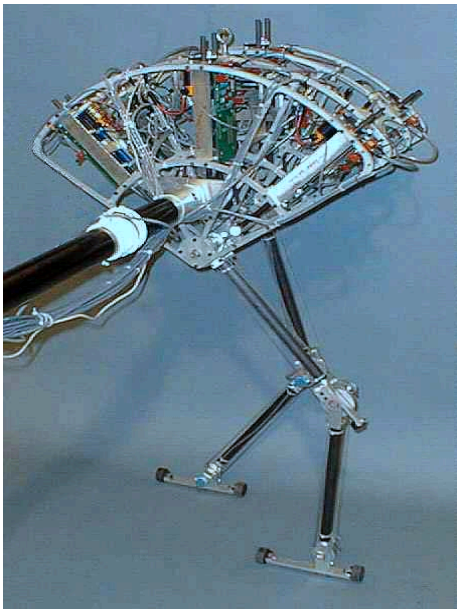

Figure 2.7: SpringFlamingo Developed in MIT Leg Lab

to investigate various walking algorithms, motion description and control techniques, particularly Virtual Model Control, force control, and actuation techniques such as Series Elastic Actuation Automatic learning techniques. The goals of M2 are to realize fast walking at a speed of 1.0 meter/second with a large margin of stability and be robust to small disturbances (reasonable pushes). They want M2 to be a "robotic workhorse" - a robot which can be reliably used to perform experiments without breaking.

2.2 Walking algorithm

Bipedal walking can be classified into static walking and dynamic walking. Different kinds of control algorithm are utilized in biped walking control: model-based, ZMP

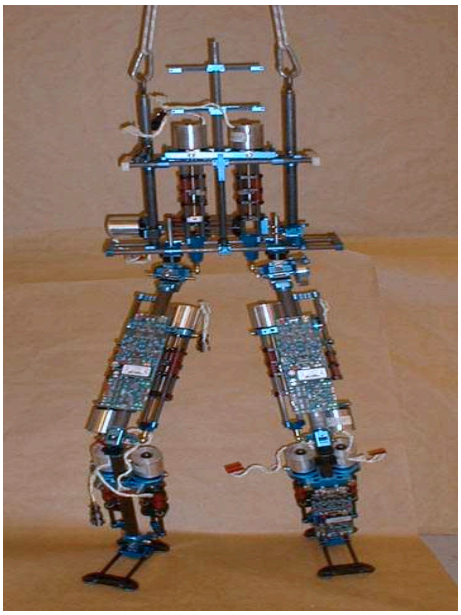

Figure 2.8: M2 3-D Biped Robot Developed in MIT Leg Lab

based, trajectory based, biologically inspired, impedance control, Virtual Model Control, etc. Each algorithm has its own advantage and sometimes synthesizing two or more algorithms can achieve better result.

Zheng et al. have synthesized the walking algorithm for static walking. Shih [27] has proposed a static walking algorithm for rugged terrain by controlling the COG. Kajita [2] studied the dynamic walking control of a biped robot along a potential energy conserving orbit. Jong [13] proposed a method based on impedance control and impedance modulation.

Pratt, et al. exploited the natural dynamics in the control of a planar and a 3-D biped walking robot [6]. A simple control algorithm is utilized to generate smooth and natural looking gait. Pratt, et al. proposed an algorithm based on the Virtual

Model Control [12]. This algorithm requires no extensive sensory system for the biped robot and enables the robot to walk blindly up and down the slopes and over rolling terrain.

Kajita and Tani use a "Linear Inverse Pendulum Model" to realize the walking on rugged terrain [14]. In this work, two experiments are carried out: the support phase experiment and the support exchange experiment. As a result, they found that a smooth leg support exchange is achieved by making the foot contact the ground with a certain vertical speed and holding two-leg support phase for a certain short period. As reported by the authors, the robot can walk over a box of 3.5 cm height at the speed of 20 cm/s.

Shih's work [5] discusses the static walking assuming that the foot angle is constant. Huang's work [17] improved the foot control by using cubic polynomial. However the position control (trajectory control) of foot angle induces large ground impact force. Further more, using the cubic polynomial to control the ankle joint requires that the profile of the landing area is exactly known. Torque control can be used on the ankle joint to adapt to the terrain.

Chapter 3

Mechanical Design and Actuators

The characteristic of dynamic motion of biped robot are closely related with its mechanical structure. In order to achieve desired performance like human beings, a good mechanical design following human body structure is required first. The mechanical design includes the length of the body and each limb. The size of the foot is also closely related to the walking performance. If the foot size is very large, the robot can easily achieve static walking. On the other side, the large foot size may make the dynamic walking difficult to realize to some extent. In order to solve this contraction, a foot with a passive toe joint is used in the mechanical design. For static walking, the robot can be regarded having a large foot. In the dynamic walking, the toe joint could be bent and the foot size becomes small. The height of the ankle joint is also crucial to bipedal walking. Sometimes the ankle joint has to be designed with a large height because of the difficulty in housing the actuator. This greatly reduces the torque that the ankle joint can provide when the ankle joint is not 90 degree. The closer the ankle joint is to the ground, the larger torque the ankle joint can provide.

The distance between the two feet is also a factor that affects walking. If the distance between the two feet is very large, the robot has to move a lot in order to move the mass center. Otherwise, the robot must walk at a high frequency. So the distance between the two feet should be small while still wide enough to avoid collision.

The mechanical design can be divided into three phases:

1. Study the structure of human body and determine the specifications of the biped robot.

2. Select the materials and components to satisfy the desired specifications.

3. Comprehend the characteristics and specifications of the components and design the architecture details.

3.1 Analysis of body structure

The weight and the weight distribution are crucial issues which should be regarded in the mechanical design. Most of the components of the robot are made of metal. Normally the weight of a robot of the same size of a human is much heavier than humans. This severely affects the dynamic performance of biped robot. It also requires higher torque actuators. Another problem in the design is the dimension ratios of body and limbs. This includes the mass and length ratios of body, trunk, thigh and calf, and the length ratio of heel and toe. All the ratios together determine the kinematics and dynamic characteristic of the robot. Trying to follow the structure of the human body is a principle in our design although it was difficult to satisfy all

the conditions. The developed robot (Robosapien) has a height of 46 cm and weights about 2 kg. The specifications of mass and dimensions for human being are listed in Table 3.1 and that for RoboSapien is in Table 3.2:

Table 3.1: Height and mass ratios of human body.

	Trunk	Thigh	Shank	Foot
Height ratio	27.8%	26.9%	26.9%	4%
Mass ratio	40%	30%	15%	10%

Table 3.2: Height and mass ratios of RoboSapien.

	Trunk	Thigh	Shank	Foot
Height ratio	28%	25%	25%	8%
Mass ratio	40%	30%	15%	10%

From the view point of kinematics, too many joints cost more and consequently make the control system more complicated; too few joint could not achieve the desired walking motion. An appropriate choice would be that enabling the robot to realize most of the walking motions that human beings can do. Figure 3.1 shows the final design of the robot links, joints and freedom.

3.2 Selection of the material and actuators

The size of the biped robot is small. All the components should be compact and the structure material should be light and strong. Aluminium alloy is chosen as the material for the body frame.

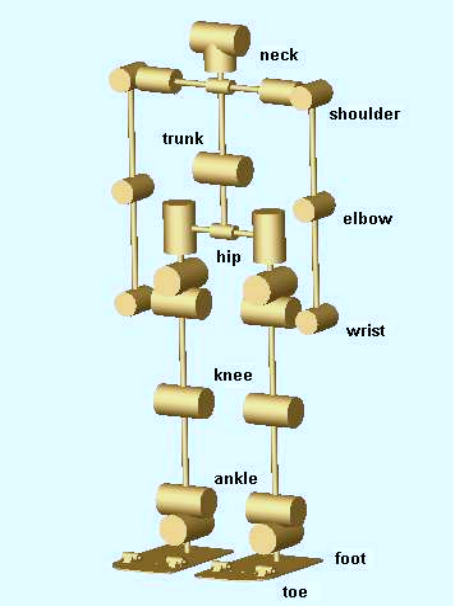

Figure 3.1: Kinematics arrangement of RoboSapien

After carefully calculating the required torque of each joint of the robot, a kind of compact and high torque digital DC servo motor is chosen as joint actuator. The digital servo provides constant high torque compared to the analog one. This servo motor has a built-in PID controller and a reduction gear box. Pulse-Width Modulation (PWM) signal is used to control the joint position. A potentiometer offers the position feedback signal. The specifications of this motor are listed in Table 3.3. The motor has only one shaft, and a new cover with shaft is designed to replace the original one. This greatly increases the stability of the whole system. The new cover, original motor and the modified motor are shown in Figure 3.2.

Figure 3.2: The motor cover, original motor and modified motor

3.3 Structural design

The objective of the structural design is to position the actuators and components satisfying all the desired specifications including the kinematics and dynamic requirements. To satisfy the requirements, a simple and light structure is opted for the legs. The design and mechanical structure of the legs are shown in Figure 3.3. Two additional DOF on the toe are designed following the structure of the human toe (Figure 3.4). However, there are no actuators on those DOF. Springs control the toe joints passively.

Figure 3.5 shows the mechanical parts of the robot legs and feet. All the parts are made of aluminium alloy.

Table 3.3: Specifications of Actuators

Motor data	value
Control Signal	+Pulse Width Control 1500usec Neutral
Operating Voltage	4.8-6.0 Volts
Operating Temperature Range	-20 to +60 Degree C
Operating speed	0.13sec/60 degrees at no load
Stall torque	13kg.cm
Current Drain (6.0V)	3mA/idle and 230mA no load operating
Dead Band Width	1usec
Gear Type	3 Metal Gears, 1 Resin Gear
Bearing Type	Dual Ball Bearing
Position Sensor	Potentiometer
Dimensions	39.4 x 20 x 37.8mm
Weight	56g

3.4 Upper body design

The upper body includes the framework to fix all the components and the cover. Figure 3.6 shows the framework. Two DSP boards, one video camera, one digital compass and one battery are fixed on the framework.

The cover of upper body (Figure 3.7)is used only to beautify the robot and protect the components.

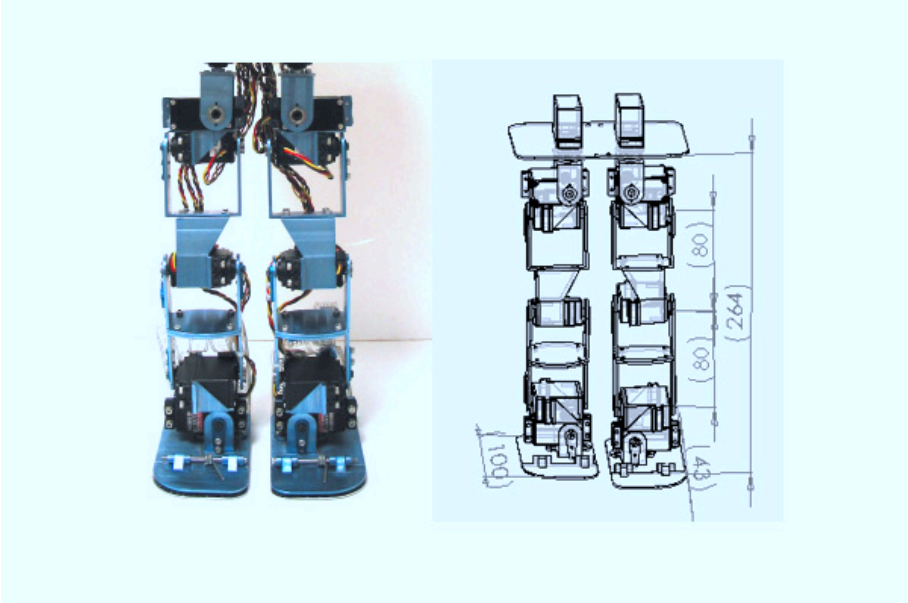

Figure 3.3: Mechanical design of legs

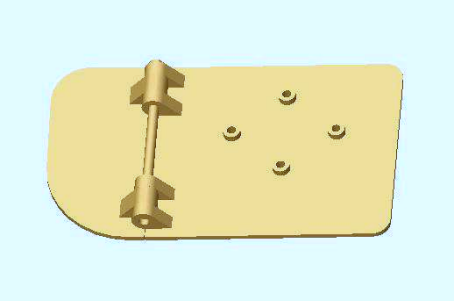

Figure 3.4: The foot design

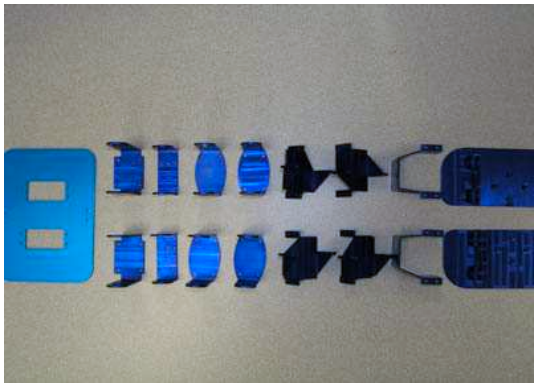

Figure 3.5: Mechanical part of legs and feet

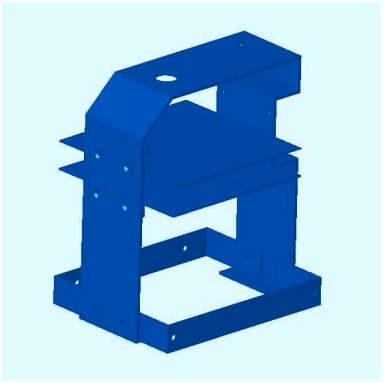

Figure 3.6: Body frame

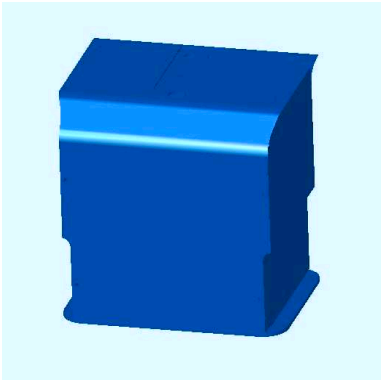

Figure 3.7: Cover of upper body

Chapter 4

Sensors Integration and Control System Configuration

4.1 Sensors

In order to perceive the environment, various sensors are equipped on the robot including video camera, digital compass, Infra-red sensor, force sensor and tilt sensor.

4.1.1 Force sensor

Eight flexible force sensors (Figure 4.1) are used on the biped robot's feet to detect the ground reaction force. The four sensors are fixed on the four corners of each sole. A simple amplification circuit is used to drive the sensor.

With its paper-thin construction, flexibility and force measurement ability, the force sensors can measure force between two surfaces and is durable enough to stand up to

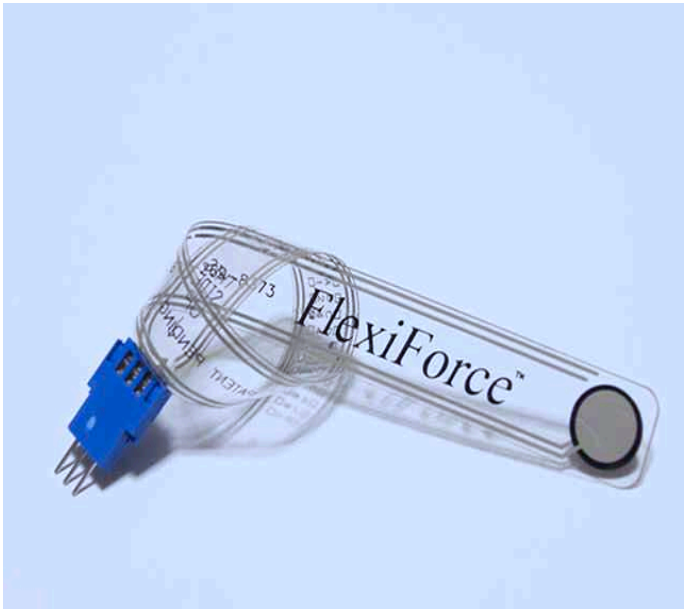

Figure 4.1: Flexible force sensor

most environments. It has good force sensing properties: linearity, hysteresis, drift and temperature sensitivity.

The force sensor is an ultra-thin (0.008”), flexible printed circuit. It is 0.55” (14 mm) wide and 8” (203 mm) in full length. The active force sensing area is a 0.375” diameter circle at the end of the force sensor. The force sensors are constructed of two layers of substrate, such as a polyester film. On each layer, a conductive material (silver) is applied, followed by a layer of pressure-sensitive ink. Adhesive is then used to laminate the two layers of substrate together to form the force sensor. The active sensing area is defined by the silver circle on top of the pressure-sensitive ink. Silver extends from the sensing area to the connectors at the other end of the sensor, forming the conductive leads. The two outer pins of the connector are active and the center pin is inactive.

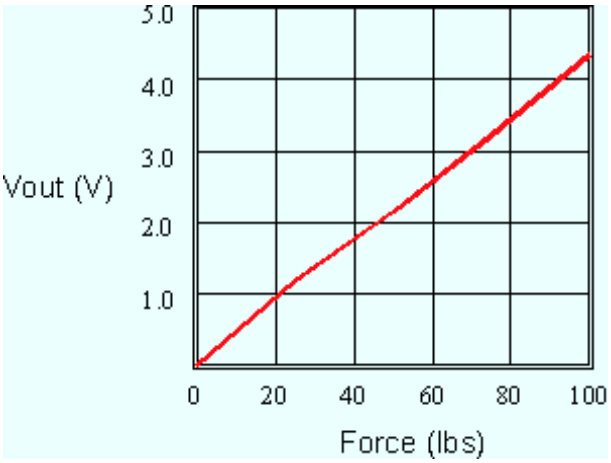

Figure 4.2: The response of force sensor

The single element force sensor acts as a force sensing resistor in an electrical circuit. When the force sensor is unloaded, its resistance is very high. When a force is applied to the sensor, this resistance decreases. The resistance can be read by connecting the outer two pins of the sensor connector to the A/D port of the controller and applying a force to the sensing area. The response property is shown in Figure 4.2.

There are many ways to integrate the force sensor into an application. One way is to incorporate it into a force-to-voltage circuit. A means of calibration must then be established to convert the output into the appropriate contact force. Depending on the setup, adjustments could then be done to increase or decrease the sensitivity of the force sensor.

Figure 4.3: Tilt sensor

4.1.2 Tilt sensor

A tilt sensor (Figure 4.3) is fixed on the upper body of RoboSapien. This tilt sensor has two axes and it is used to detect the tilt angles in the sagittal and lateral planes. However, when the body undergoes acceleration, the angle measured by the tilt sensor is not the same as the actual tilt angle. An accelerometer can be utilized to compensate such an error.

4.1.3 Digital compass

For navigational purposes, a digital compass (Figure 4.4) is fixed on to RoboSapien. Direction information is very important to realize certain tasks. The digital compass provides direction information based on the earth magnetism and navigates the robot

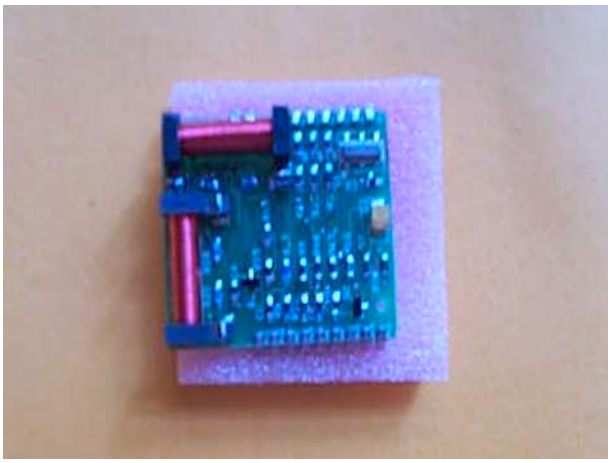

Figure 4.4: Digital compass

to accomplish the assigned tasks. The compass has an accuracy of 2^o and a resolution of 1^o. The compass communicates with the DSP boards via PWM signals. The working of the digital compass depends on the magnetic field of the earth. The compass should be placed away from any electromagnetic components such as motors.

4.1.4 Video camera

A CMU camera [28] is used as the eye of the robot. With the video camera (Figure 4.5) the robot can track a specified object. Driven by two servo motors, the camera can turn about the horizontal and vertical axes. It has a built in processor to process the image and determine the position information of the object in front of the robot. The position information of the object is sent to the controller through the serial port.

At 17 frames per second, the CMUcam can do the following:

(1) Track the position and size of a colorful or bright object.

(2) Measure the RGB or YUV statistics of an image region.

(3) Automatically acquire and track the first object it sees.

(4) Physically track using a directly connected servo.

(5) Dump complete image over the serial port.

(6) Dump a bitmap showing the shape of the tracked object.

The camera dimensions are 2.25" wide x 1.75" high x 2" deep. The camera kit uses a Omnivision OV6620 single-chip CMOS CIF color digital camera with a 4.0 mm, F2.8 lens and IR filter.

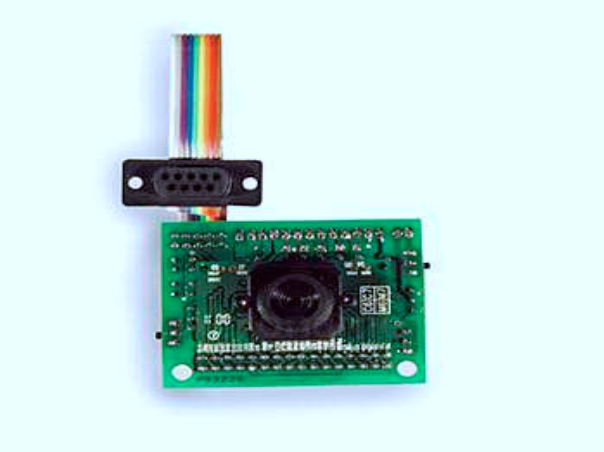

Figure 4.5: Video camera

4.1.5 IR sensor

An Infra Red (IR) sensor fixed on the robot body can detect obstacles even under poor lighting conditions. This sensor (Figure 4.6) takes a continuous distance reading and reports the distance as an analog voltage with a distance range of 10cm (4") to 80cm (30"). The interface is 3-wire with power, ground and the output voltage.

Figure 4.6: Infra Red Sensor

When the robot walks, the IR sensor rotates around the vertical axis scanning from left to right, to detect obstacles in the path of the robot. This idea comes from the Radar system. Such an arrangement reduces the number of IR sensors (otherwise, several sensors should be used around the robot) and saves the system resource such as A/D port. One the other hand, it provides the obstacles' position and distance information at any angle within its scanning range. This improves the capability of the robot in detecting obstacles and planning the path.

4.1.6 Controller

Digital Signal Processors (DSP) Motorola 56F805 and 56F807 are used as the high level controller and low level controller respectively. The DSP board (Figure 4.7) has the following specifications:

Programming language Isomax, Small C, Assembly or Forth.

DSP56F807 MPU, 16-bit processor

Up to 40 MIPS at 80 MHZ core frequency

Extensive on-chip Flash w/100,000 write cycles (typical)

60K x 16-bit words Program Flash

8K x 16-bit words Data Flash

2K x 16-bit words Program ram

4K x 16-bit words Data Ram

Serial Peripheral Interface (SPI)

Two Serial Communication Interface (SCI)

CAN 2.0 A/B module

Two 8-channel 12-bit ADCs

12-channel PWM module

4.2 Control system configuration

The control system structure of RoboSapien is shown in Figure 4.8. The system is divided into two parts: a high level control part and a walking control part. Digital Signal Processors (DSP) Motorola 56F805 and 56F807 are used as the controllers. The two DSPs communicate through a Serial Peripheral Interface (SPI). The high level control DSP receives the video camera signals via serial port. The camera provides

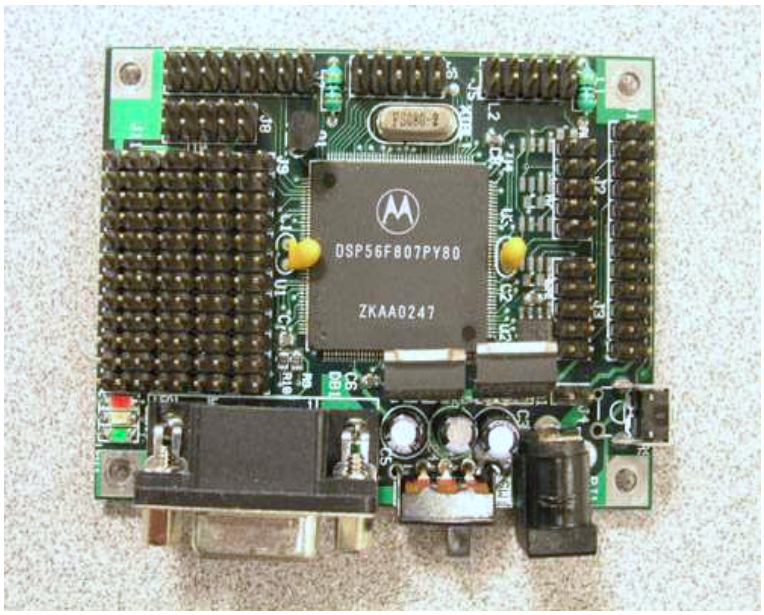

Figure 4.7: Controller

the position information of an object within a specified color range. The DSP reads the IR sensor's signal to obtain the obstacle's distance and position information. The DSP also receives the output from the digital compass. The compass provides the direction information. In accordance with the the information from the sensors, the DSP makes decisions and commands the low level DSP for walking control. The DSP for high level control is also used to control the DC servo motors to drive the camera and IR sensor.

The walking control DSP is used as a low level controller to control walking and other actions, like kicking a ball. The lower level DSP receives commands from the higher level DSP. Signals from tilt sensor and eight force sensors are sent to the lower level DSP via A/D ports. Based on the sensor information and higher level commands the walking motion and other actions are generated. The lower level DSP controls

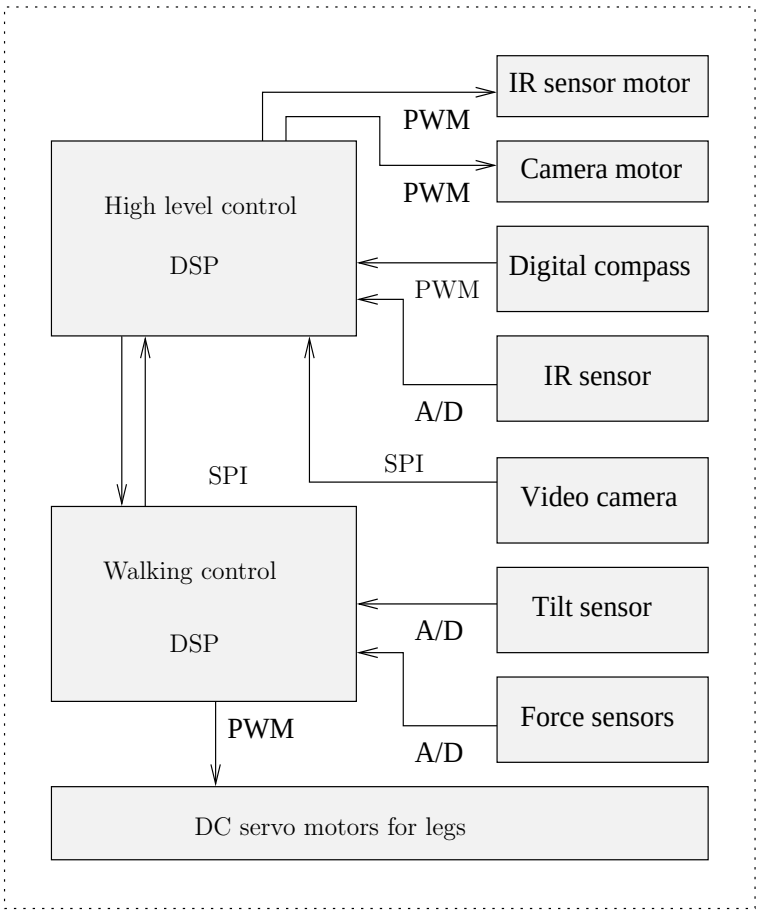

Figure 4.8: Control system configuration

the DC servo motors on the legs with appropriate PWM signals. After the desired positions are generated by the walking control algorithm, the position information is sent to the DC servo motors.

Chapter 5

Trajectory Based Walking Algorithm

The walking algorithm proposed in the thesis can realize dynamic walking on flat ground, rough terrain and, even up and down stairs. Besides, this algorithm enables the robot to start walking in a random phase of walking. Walking motion of biped can be determined by the hip trajectory and the swing foot trajectory. ZMP (Zero Moment Point) is the point on the ground around which the sum of all the moments of the active forces equals zero. The stability can be characterized by the ZMP criterion.

The sagittal motion control algorithm includes the following steps:

(i)For each step, the desired final state, speed and position of hip and swing foot (v_{xhe}, v_{zhe}), (v_{xfe}, v_{zfe}), (x_{he}, z_{he}), (x_{fe}, z_{fe}) and step length L_s (Figure 5.5) are specified.

(ii)The desired θ_e (Figure 5.6) is specified. The hip height adapting to the terrain is

derived using the optimal hip height principle (5.9).

(iii)The hip and foot trajectories are generated for the two parts of a single support period (T_1 and T_p) (5.15).

(iv)Change the parameters and repeat step i, ii, iii. The trajectory with satisfied ZMP trajectory is selected.

(v) The desired state at the beginning of a walking cycle is derived by *Lemma 5.1.*

(vi)The double support phase drives the robot into the desired initial state.

5.1 Single and double support phase

A walking cycle can be divided into single support phase and double support phase. As shown in Figure 5.1, from point 1 to 2 is the single support phase and from point 2 to 3 is the double support phase. In the single support phase, the support foot is stationary on the ground. The other foot swings from the back to the front. The hip also moves along a trajectory. The double support phase starts from the forward foot touching the ground and ends with the rear foot leaving the ground. During the double support phase, the weight transfers from the rear foot to the forward foot. This phase is known as weight acceptance phase [13].

In order to achieve continuous dynamic walking, the transfer between single support phase and double support phase should be smooth. Normally at the beginning of double support phase, the impact when the forward foot contacts the ground is very large and affects the walking stability. To solve this problem, force feedback control

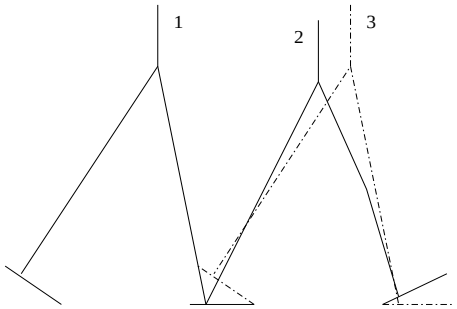

Figure 5.1: Walking cycle: single and double support phase

is used.

5.2 ZMP and ankle torque

The ZMP is the point on the ground around which the sum of all the moments of the active forces equals zero. Under the assumption that no external force exists, the ZMP can be computed by [17]:

$$x_{zmp} = \frac{\sum_i m_i(\ddot{z}_i + g)x_i - \sum_i m_i\ddot{x}_i z_i - \sum_i I_{iy}\ddot{\theta}_{iy}}{\sum_i m_i(\ddot{z}_i + g)} \tag{5.1}$$

$$y_{zmp} = \frac{\sum_i m_i(\ddot{z}_i + g)y_i - \sum_i m_i\ddot{y}_i z_i - \sum_i I_{ix}\ddot{\theta}_{ix}}{\sum_i m_i(\ddot{z}_i + g)} \tag{5.2}$$

where $(x_{zmp}, y_{zmp}, 0)$ is the coordinate of the ZMP, (x_i, y_i, z_i) is the mass center of link i on a Cartesian coordinate system. m_i is the mass of link i, g is the gravitational acceleration. I_{ix} and I_{iy} are the inertia components, $\ddot{\theta}_{iy}$ and $\ddot{\theta}_{ix}$ are the angular speed around axis y and x about the center of mass of link i. (Figure 5.2)

As shown in Figure 5.3, for the sagittal plane, the ZMP can be derived directly

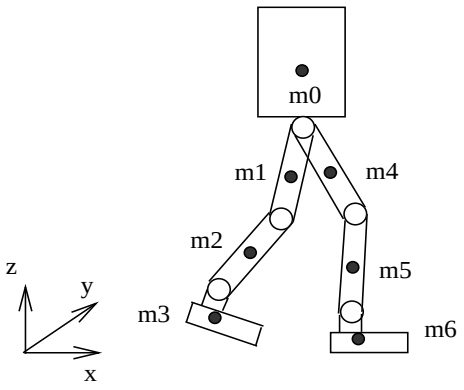

Figure 5.2: Biped robot model

through dividing the ankle torque by reaction force:

$$x_{zmp} = \frac{\tau_x}{\sum_i m_i(\ddot{z}_i + g)} \tag{5.3}$$

Therefore, the ankle torque can be written as:

$$\tau_x = x_{zmp} \cdot \sum_i m_i(\ddot{z}_i + g) \tag{5.4}$$

For stable dynamic walking the range of the ZMP should be in the convex of the contact points between the foot and the ground. The range of x_{zmp} can be written as:

$$x_{zmp} \in \{S | S \in R, S \in (-x_a, x_b)\} \tag{5.5}$$

Suppose the robot has a point mass at the hip and the support knee joint angle is kept constant then an inverted pendulum model can be used. The length of leg is L, $\tau_{xa}(\theta)$ and $\tau_{xb}(\theta)$ are respectively the maximum and minimum ankle torques in the sagittal plane. Then the relation can be represented by:

$$\tau_{xa}(\theta) = m(g + (\frac{\tau_{xa}(\theta)}{Lm} - gsin\theta)sin\theta - \frac{v^2}{L} \cdot cos\theta)x_a \tag{5.6}$$

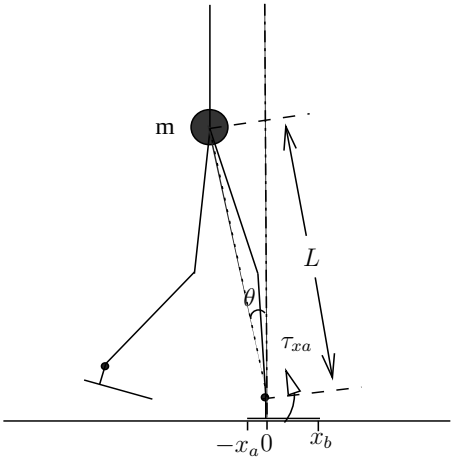

Figure 5.3: Invert pendulum model to derive the ankle torque

where v is the velocity of the hip and $\frac{v^2}{L}$ is the centripetal acceleration. $(\frac{\tau_{xa}(\theta)}{Lm} - gsin\theta)sin\theta - \frac{v^2}{L} \cdot cos\theta$ is the $\ddot{z}$ in (5.4). The centripetal acceleration is much smaller than the other components so that it can be neglected in (5.6), and the ankle torque can be described as:

$$\tau_{xa}(\theta) = \frac{mgx_a(1 - sin^2\theta)}{1 - \frac{sin\theta}{L}x_a} \tag{5.7}$$

Similarly,

$$\tau_{xb}(\theta) = \frac{mgx_b(1 - sin^2\theta)}{1 + \frac{sin\theta}{L}x_b} \tag{5.8}$$

As for the biped robot RoboSapien, these parameters are: $m = 3kg$, $x_a = 0.0248m$, $x_b = 0.0552m$, $\theta \in \{ß|ß \in R, ß \in (-45^0, 60^0)\}$, $L = 0.20m$. Figure 5.4 shows the ankle torque range when the ZMP is within the stable region in sagittal plane.

Under the assumption that the support knee joint angle is kept constant, the range of the ankle torque to keep the ZMP in the support region is derived. This result is used in section (5.5) to approximate the desired initial state of walking cycle. This

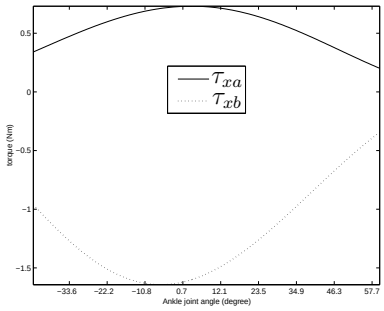

Figure 5.4: Ankle torque range when the ZMP in the stable region

range of ankle torque also provides a rough idea on choosing actuators during the mechanical design.

5.3 Hip trajectory for single support phase

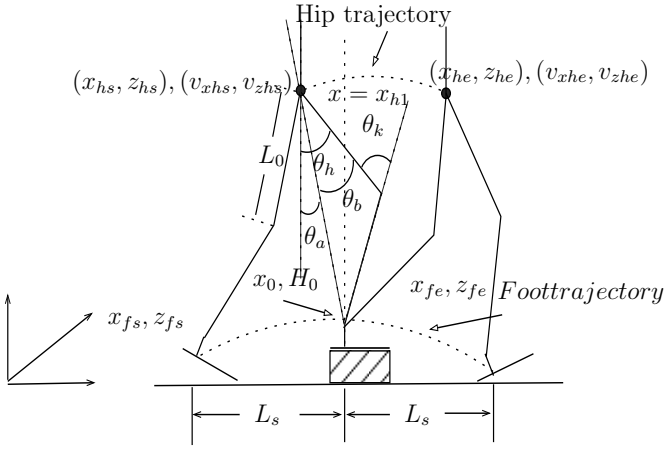

Figure 5.5: Hip and foot trajectory

As shown in Figure 5.5, hip trajectory can be generated by cubic polynomial if the

initial and final states are known for single support phase. The initial state is known and the final state includes $[x_h, z_h]^T$ and $[v_{hx}, v_{hz}]^T$. The desired $[v_{hx}, v_{hz}]^T$ is specified.

In order to adapt to various terrains, the supporting knee should be able to bend so that it can achieve the desired hip height z_h. For example, if the robot is walking up a stair, it should try to lift the hip to a maximum height. On the contrary when it is descending a stair, it should try to lower the hip to enable the foot to reach the lower stair. If the step length L_s in Figure 5.5 and angle θ_e in Figure 5.6 are specified, a principle to determine the hip height is proposed:

$$z_h = min(max(h_s), max(h_l)) \tag{5.9}$$

where h_s and h_{sm} are respectively the possible and maximum hip heights for the

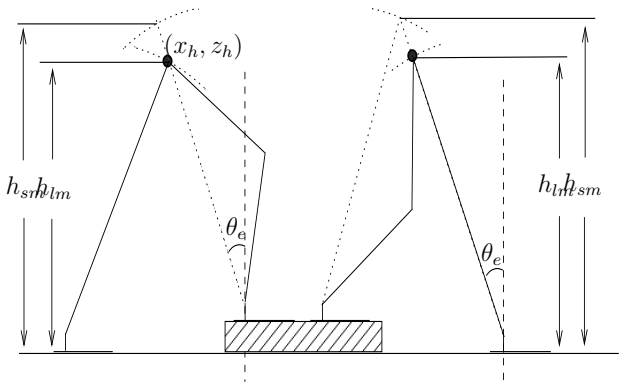

Figure 5.6: Determine the height of hip

support leg, h_l and h_{lm} are respectively the possible and maximum hip heights for the land leg at the beginning of double support phase (Figure 5.6). This criterion can provide an reasonable hip height no matter whether the next land point is higher

or lower than the current land point. The hip position along x direction (x_h) can be derived as shown in Figure 5.6.

Since the initial state is known and the desired final state is achieved, the hip trajectory for single support phase can be generated by cubic polynomial. The initial and final constraints of cubic trajectory for z direction $z_h(t)$ can be described as:

$$z_h(t) = \begin{cases} z_{hs} & \text{if } t = kT \\ z_{he} & \text{if } t = kT + T_s \end{cases} \tag{5.10}$$

where T is the period for one step and T_s is the period for single support phase.

$$\dot{z_h}(t) = \begin{cases} v_{zhs} & \text{if } t = kT \\ v_{zhe} & \text{if } t = kT + T_s \end{cases} \tag{5.11}$$

The cubic polynomial

$$z_h(t) = a_0 + a_1 t + a_2 t^2 + a_3 t^3 \tag{5.12}$$

with four parameters a_0, a_1, a_2 and a_2 satisfies the initial and final constraints. Substituting (5.10) and (5.11) into (5.12), the four parameters can be derived and the cubic polynomial can be written as:

$$\begin{aligned} z_h(t) = & z_{hs} + v_{zhs}(t-kT) + \frac{3(z_{he}-z_{hs}) - 2v_{zhs}T_s - v_{zhe}T_s}{T_s^2}(t-kT)^2 \\ & + \frac{2(z_{hs}-z_{he}) + (v_{zhs}+v_{zhe})T_s}{T_s^3}(t-kT)^3 \end{aligned} \tag{5.13}$$

$$kT < t \leq kT + T_s$$

$x_h(t)$ is divided into two parts: $x_h(kT)$ to $x_h(kT+T_1)$ and $x_h(kT+T_1)$ to $x_h(kT+T_p)$. The constraints for $x_h(t)$ are: (Figure 5.5)

$$\begin{cases} x_h(t) = x_{hs} & \text{t=kT} \\ x_h(t) = x_{h1} & \text{t=kT+}T_1 \\ x_h(t) = x_{he} & \text{t=kT+}T_p \\ \dot{x}_h(t) = v_{xhs} & \text{t=kT} \\ \dot{x}_h(t^-) = \dot{x}_h(t^+) & \text{t=kT+}T_1 \\ \dot{x}_h(t) = v_{xhe} & \text{t=kT+}T_p \\ \ddot{x}_h(t) = a_0 & \text{t=kT} \end{cases} \tag{5.14}$$

where a_0 is to be specified to satisfy the initial acceleration. The trajectory is composed of two cubic polynomials and the trajectory satisfies constraints (5.15).

The cubic polynomial trajectory can be derived as:

$$x_h(t) = \begin{cases} x_{hs} + v_{xhs}(t-kT) + \frac{1}{2}a_0(t-kT)^2 \\ +\frac{(x_{h1}-x_{hs}-v_{xhs}T_1-\frac{1}{2}a_0T_1^2)(t-kT)^3}{T_1^3} \\ \qquad kT < t \leq kT + T_1 \\ x_{h1} + v_{xh1}(t-kT-T_1) \\ +\frac{(3(x_{he}-x_{h1})-2v_{xh1}(T_2-T_1))(t-kT-T_1)^2}{(T_2-T_1)^2} \\ +\frac{(2(x_{h1}-x_{he})+(v_{xh1}+v_{x2})(T_2-T_1))(t-kT-T_1)^3}{(T_2-T_1)^3} \\ \qquad kT + T_1 < t \leq kT + T_p \end{cases} \tag{5.15}$$

where v_{xh1} can be derived from the first part of (5.15).

5.4 Swing foot trajectory for single support phase

Cubic polynomial is used to generate the swing foot trajectory of single support phase. At the starting point and ending point, the following position and speed constraints must be satisfied: (Figure 5.5)

$$\begin{cases} x_f(t) = x_{fs} & \text{t=kT} \\ x_f(t) = x_{fe} & \text{t=kT+}T_s \\ z_f(t) = z_{fs} & \text{t=kT} \\ z_f(t) = z_{fe} & \text{t=kT+}T_s \end{cases} \tag{5.16}$$

$$\begin{cases} \dot{x}_f(t) = 0 & t = kT \\ \dot{x}_f(t) = 0 & t = kT + T_s \\ \dot{z}_f(t) = 0 & t = kT \\ \dot{z}_f(t) = 0 & t = kT + T_s \end{cases} \tag{5.17}$$

Assuming that the obstacle's height is H_o and position is at x_o. In order to avoid colliding with an obstacle the height of swing foot should be larger than H_o at $x = x_o$. The constraint can be described as:

$$\begin{cases} z(t) = H_o & t = kT + T_o \\ \dot{z}(t) = 0 & t = kT + T_o \end{cases} \tag{5.18}$$

Giving the start and end positions on x and z direction, and the height of the obstacle H_o, a smooth foot trajectory $f(t) = [x_f(t), z_f(t)]^T$ can be generated as:

$$x_f(t) = x_{fs} + 3(x_{fe} - x_{fs}) \cdot \frac{(t - kT)^2}{{T_s}^2}$$

$$-2(x_{fe}-x_{fs})\cdot\frac{(t-kT)^3}{{T_s}^3}kT\le t\le kT+Ts \tag{5.19}$$

$$z_f(t)=\begin{cases} z_{fs}+3(z_{fm}-z_{fs})\cdot\frac{(t-kT)^2}{{T_m}^2} \\ -2(z_{fm}-z_{fs})\cdot\frac{(t-kT)^3}{{T_m}^3} \\ kT\le t\le kT+T_m \\ z_{fm}+3(z_{fe}-z_{fm})\cdot\frac{(t-kT-T_m)^2}{(Ts-Tm)^2} \\ -2(z_{fe}-z_{fm})\cdot\frac{(t-kT-T_m)^3}{(Ts-Tm)^3} \\ kT+Tm<t\le kT+Ts \end{cases} \tag{5.20}$$

The joint position of hip and knee of the swing leg can be derived by inverse kinematics. Suppose the hip and swing foot positions in the sagittal plane at time t are $h(t)=[x_h(t),z_h(t)]^T$ and $f(t)=[x_f(t),z_f(t)]^T$, then the inverse kinematics of the swing leg can be derived from Figure 5.5 as follows:

$$q=\begin{bmatrix}\theta_a\\ \theta_b\end{bmatrix}=\begin{bmatrix} sin^{-1}\frac{((x_f(t)-x_h(t))}{\sqrt{(x_f(t)-x_h(t))^2+(z_h(t)-z_f(t))^2}} \\ cos^{-1}\frac{\sqrt{(x_f(t)-x_h(t))^2+(z_h(t)-z_f(t))^2}}{2L_o}\end{bmatrix}. \tag{5.21}$$

As shown in Figure 5.5, $\theta_h=\theta_a+\theta_b$ and $\theta_k=2\theta_b$. θ_h and θ_k are the hip and knee joint angles respectively and L_o is the length of thigh and calf.

5.5 Double support phase control

The robot falls backward if the initial state $[x_{hs},z_{hs}]^T$, $[v_{hxs},v_{hzs}]^T$ is not suitable. The unstable period T_u is defined from the beginning of single support phase to the COG

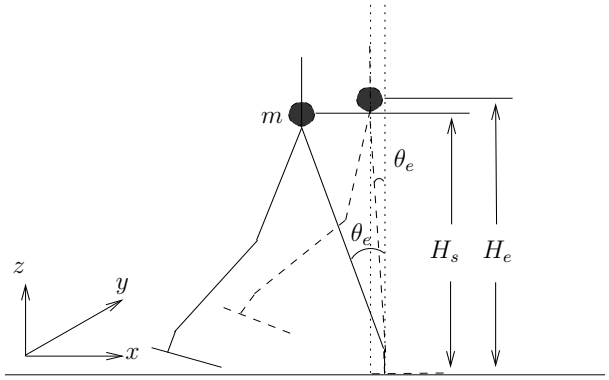

Figure 5.7: From unstable to stable region

entering the support region (Figure 5.7). From the view point of energy conservation, the following criterion can be derived:

Lemma 5.1 *When the rear foot leaves the ground, the kinetic energy should be large enough to drive the COG entering the range of the supporting region on the sagittal plane with limited control, otherwise the robot tips over. This can be represented by:*

$$\frac{1}{2}m(\dot{x}^2 + \dot{z}^2) + \int_{\theta_e}^{\theta_e} \tau_{max}(\theta)d\theta \geq mg(H_e - H_s) \tag{5.22}$$

where τ_{max} is the maximum ankle torque, I is the inertial component and $\dot{\theta}$ is the angular velocity around support ankle joint. H_e and H_s are the initial and final hip heights for unstable period as shown in Figure 5.7. It is supposed that the support knee joint angle is kept constant when the τ_{max} is derived. Consequently this is only an approximation expression when the support knee joint angle changes.

The initial state of single support phase is the final state of double support phase. The state should satisfy *Lemma 5.1.* In the double support phase, the ankle of forward leg adapts to the terrain profile and the ankle of the rear leg is used to realize the

state satisfying (5.22) by pushing the body forward and upward.

Chapter 6

Simulation and Experiment

To evaluate the performance of the walking algorithm proposed in Chapter 5, walking on flat ground and climbing stairs are simulated and the results are provided.

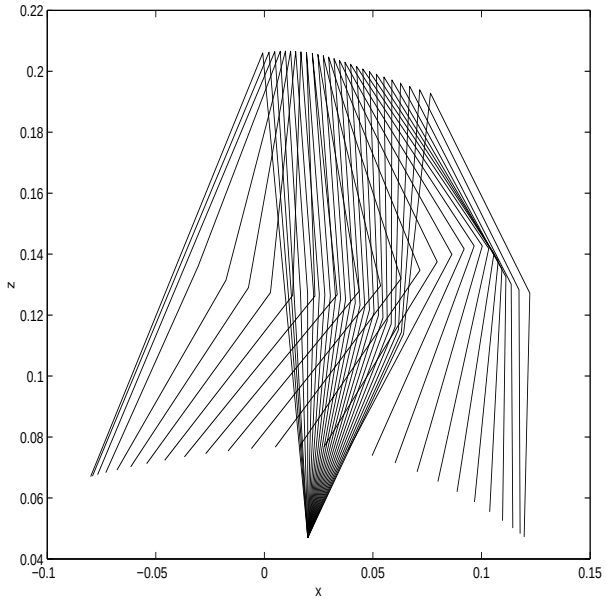

Figure 6.1: Stick diagram of gaits in single support phase for walking on flat ground

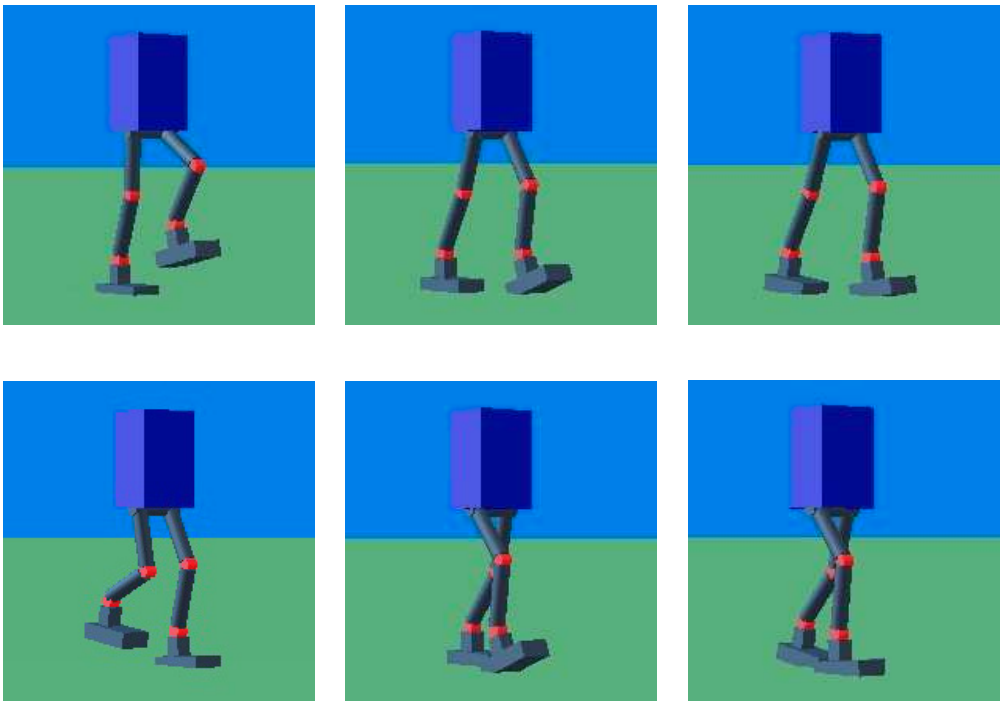

Figure 6.2: The snap shots of simulation of biped locomotion on flat ground

6.1 Simulation for flat ground

6.1.1 Gait generation

The proposed algorithm generates the desired hip trajectory and swing foot trajectory which satisfy the ZMP criterion and ground constraint. In this control algorithm the robot is not redundant in the sagittal plane. When the hip position and swing foot position are known, all the joint positions can be solved for. Figure 6.1 shows the desired gait in single support phase. In this example, the initial speed $[v_{xhs}, v_{zhs}]^T$ is $[0.1, 0.01]^T$ and the final speed $[v_{xhe}, v_{zhe}]^T$ is $[0.18, -0.03]^T$. The step length L_s is $0.115m$. The obstacle is at the middle of the step with a height H_0 of $3cm$. The hip trajectory along x axis is divided into two parts by T_1. At time $t = kT + T_1$ the speed

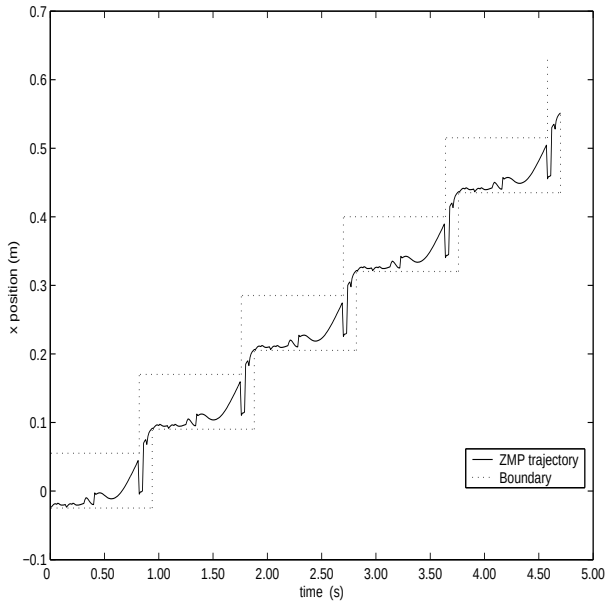

Figure 6.3: ZMP trajectory along the walking direction

should satisfy: $v^{+}_{xh1} = v^{-}_{xh1}$. As a result the velocity of hip trajectory is continuous along the x direction and the acceleration is continuous along z direction. The foot trajectory along z axis is divided into two parts by T_m. At time $t = T_m$ the speed should satisfy: $v^{+}_{zfm} = v^{-}_{zfm}$. Subsequently the speed of foot trajectory is continuous along the z direction and the acceleration is continuous along the x direction.

6.1.2 Simulation study

Yobotics simulation construction set [25] is used to simulate the locomotion of the biped robot. The robot can walk on flat and uneven ground. A nonlinear model is

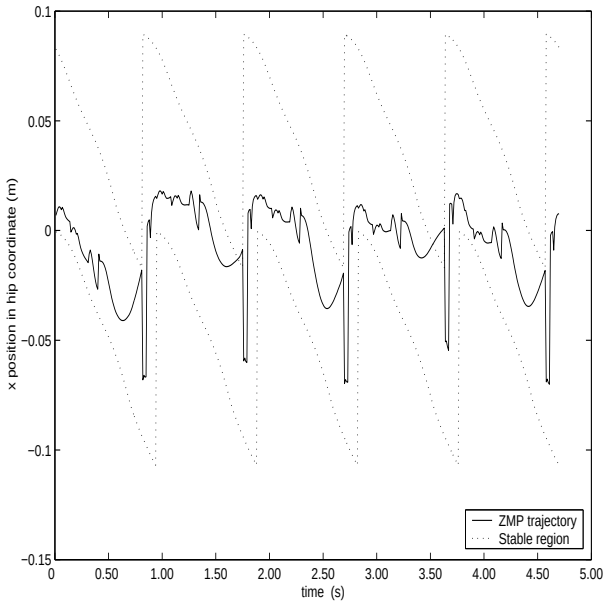

Figure 6.4: ZMP trajectory in the hip coordinate system

used as the ground contact model: [25]

$$F_z = \begin{cases} -K_z \cdot (z - z_0)/(N_l + z - z_0) + B_z \cdot \dot{z} & N_l + z - z_0 \geq C_1 \\ -K_z \cdot (z - z_0)/C_1 + B_z \cdot \dot{z} & N_l + z - z_0 < C_1 \end{cases} \tag{6.1}$$

where F_z is the ground reaction force, z and z_0 are the position of ground contact point and ground height respectively. The joint positions can be determined by the hip and swing foot trajectories. A PD controller (6.2) is used for the control of each joint.

$$\tau = K_p e - K_d \dot{q} \tag{6.2}$$

The walking cycle is divided into six stages. The robot can start walking from any initial state. In order to realize continuous dynamic walking, the initial state must satisfy *Lemma 5.1.* Figure 6.2 shows the snap shots of the biped locomotion in each

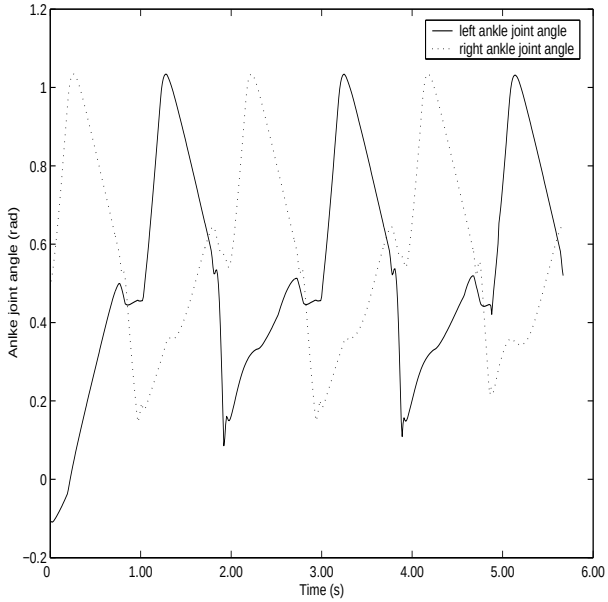

Figure 6.5: Ankle joint angle

stage. Stage 1 is the right leg single support phase. In this stage the support leg swings the body along the desired hip trajectory. The swing foot kinematic motion has been decoupled with the support leg motion. The swing foot follows a desired trajectory with reference to the ground. The trajectory avoids the obstacles by giving a maximum height H_0 at the desired position $x = x_0$ (Figure 5.5). Stage 2 is the forward falling phase. In this stage the robot falls forward to enable the heel of land foot to reach the ground. Stage 3 is the double support phase. In this phase, local force feedback control is used to reduce the landing impact. At the same time the former support leg pushes the robot body to the desire position and speed to prepare for the next single support phase. The working procedures for stages 4, 5, and 6 (left leg support) are respectively similar to stages 1, 2 and 3 (right leg support).

Figure 6.3 shows the ZMP trajectory along the walking direction. Figure 6.4 shows

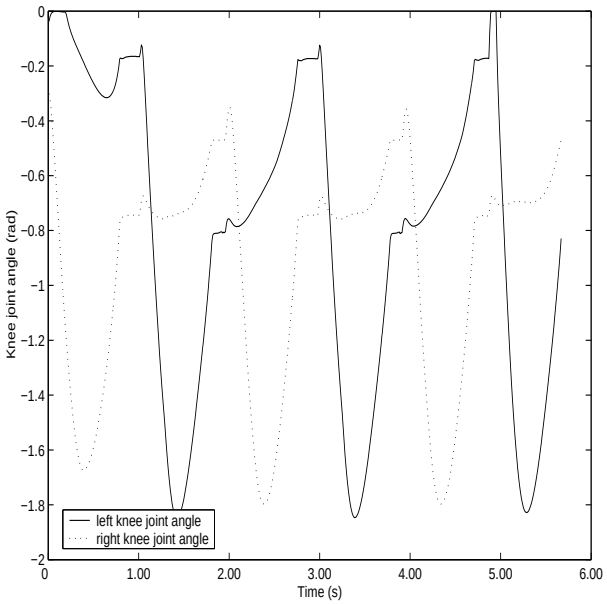

Figure 6.6: Knee joint angle

the ZMP trajectory in the hip coordinate system.

Figures 6.5, 6.6 and 6.7 show the joint angles of ankle, knee and hip. Figures 6.8, 6.9 and 6.10 show how the hip joint velocity $\dot{q_h}$ changes with the hip joint position q_h. The trajectory converges to a limit cycle with time passing by, which proves the stability of the locomotion. Figures 6.8, 6.9 and 6.10 show different initial states and prove that the robot can start walking from any initial state satisfying certain constraints (*Lemma 5.1*).

Figure 6.11 shows the real biped robot walking on flat ground.

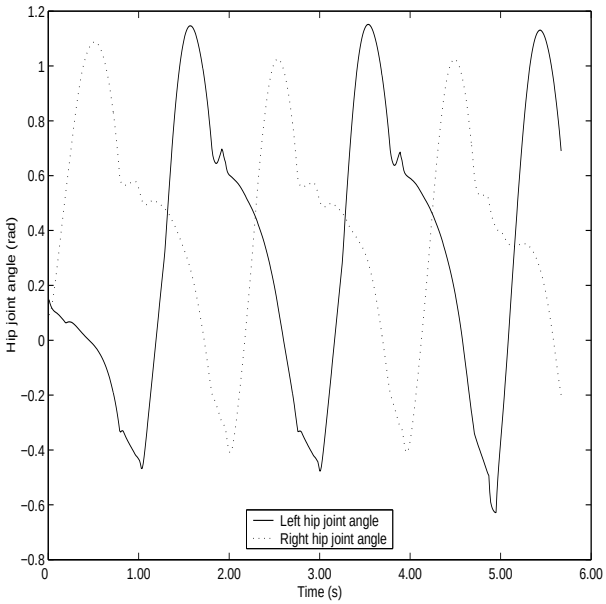

Figure 6.7: Hip joint angle

6.2 Simulation for climbing stairs

As mentioned in Chapter 1, the objective is to synthesize a walking algorithm which can adapt to flat ground, rough terrain and even stairs. This section tests whether the robot can climb up stairs using the same algorithm.

Various parameters are used in the trajectory generation. For climbing the stairs, the position should satisfied the constraints, $z_{fe} = z_{fs} + 2S_h$, $x_{fe} = x_{fs} + 2L_s$ (Figure 6.12).

The gait for climbing up stairs is shown in Figure 6.13.

The simulation of the climbing (Figure 6.14) shows that the robot is able to climb up the stairs. Stable climbing motion is realized by just changing the two parameters

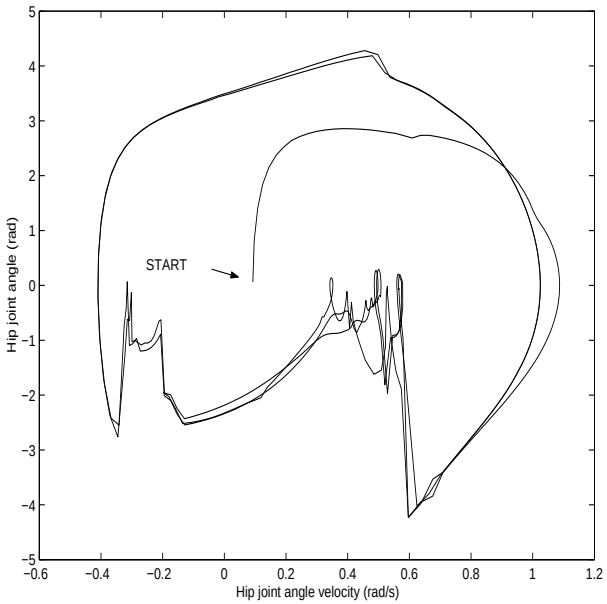

Figure 6.8: The position and velocity of hip joint converge to a limit cycle: initial state A

z_{fe} and x_{fe} (Figure 6.12) in the walking algorithm. This proves that the walking algorithm can realize the walking on uneven terrain.

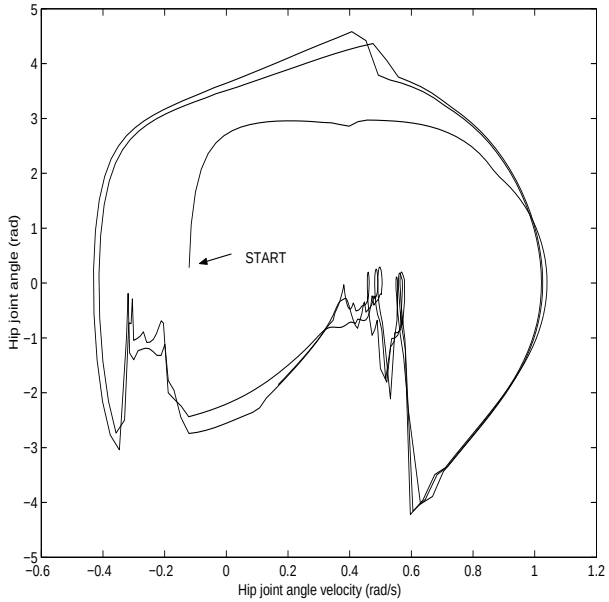

Figure 6.9: The position and velocity of hip joint converge to a limit cycle: initial state B

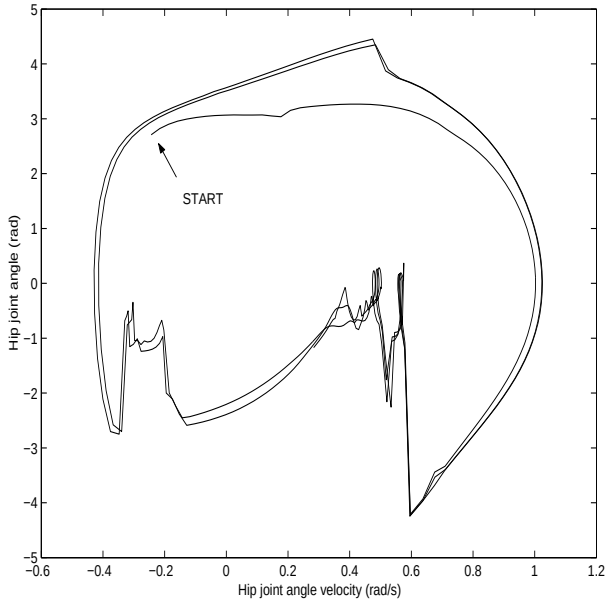

Figure 6.10: The position and velocity of hip joint converge to a limit cycle: initial state C.

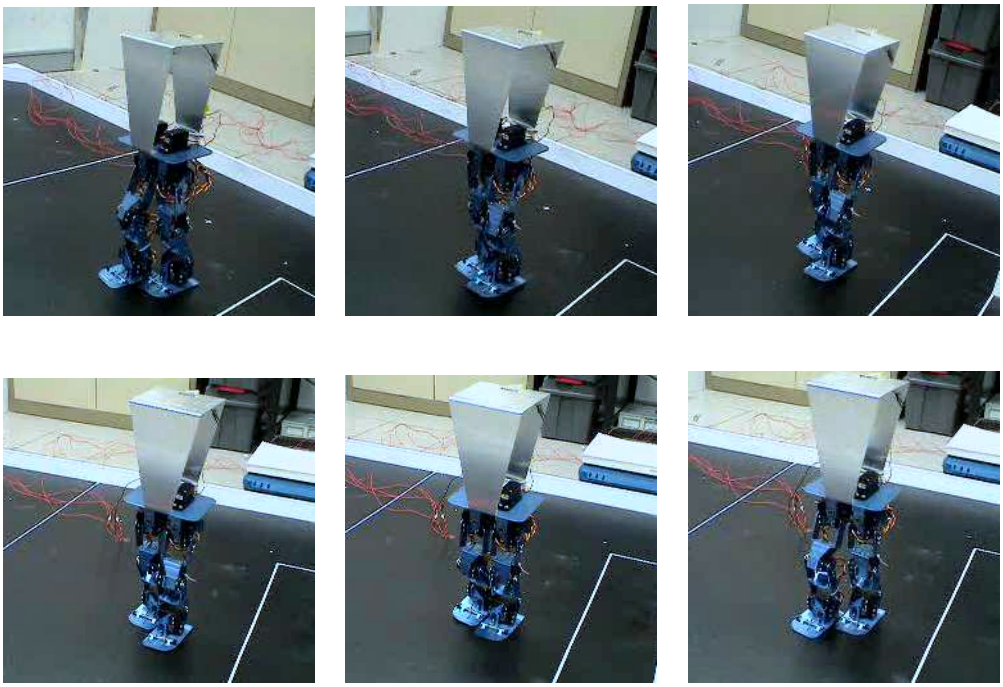

Figure 6.11: Biped robot walking on flat ground

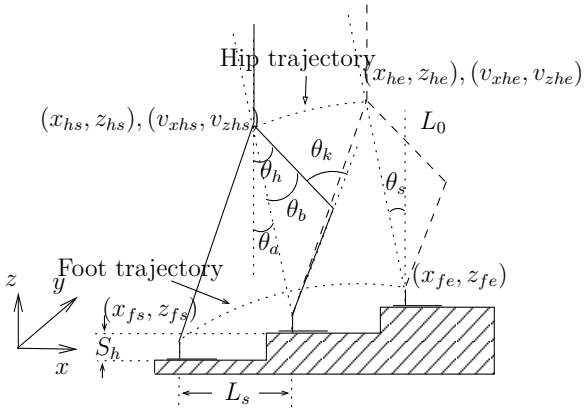

Figure 6.12: Hip and foot trajectory for climbing stairs

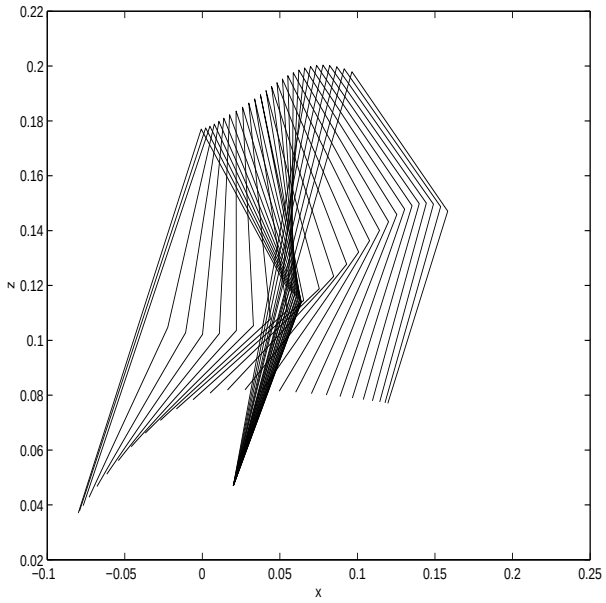

Figure 6.13: Stick diagram of gaits in single support phase for climbing up stairs.

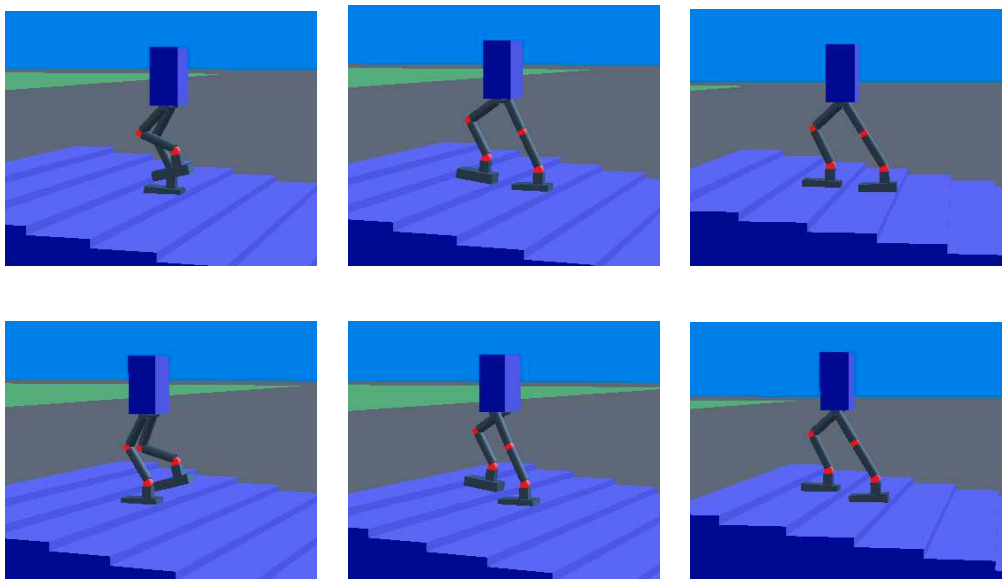

Figure 6.14: The simulation snap shots of biped locomotion climbing stairs

Chapter 7

Evolution of the Trajectory Based Algorithm

7.1 Evolutionary algorithm

Evolutionary algorithms (EA) [29] are stochastic search techniques based on natural selection and the survival of the fittest. Nature produces a population with individuals that fit the environment better. By mimicking this concept, EA are successfully used in various fields. In EA, each individual represents a search point in the space of potential solution of a given problem. Descendants of individuals are generated by randomized processes intended to model recombination and mutation. Recombination exchanges information between two or more parent individuals, and mutation corresponds to an erroneous self-replication of individuals. To evaluate the performance of each individual, a fitness value is assigned to individuals. The probability of

the individual to be selected as a parent depends on the fitness value. The individual with a better fitness value has more chance to be selected. This ensures that good quality is inherited by the following generation.

Evolutionary algorithms are also useful to generate optimal robot walking sequences. Some applications [30, 31] on robot motion control are very successful. This chapter describes an evolutionary algorithm for planning motion patterns for the biped robot. Evolutionary algorithm is utilized to search for the combination of parameters that can result in the best performance.

In the gait generation algorithm, introduced in the Chapter 5, there are various parameters to tune to. This process is complicated and normally the best performance can not be achieved always. This part introduces an evolutionary algorithm for turning the parameters.

In evolutionary algorithms, strings and characters are used to simulate chromosomes and genes. An evaluation function or fitness function $F(t)$ is defined to evaluate the performance of each gene combination. The ideas of population, generations, reproduction, crossover and mutation are also used to simulate a natural system. The reproduction genetic operation is based on the Darwinian principle of reproduction and survival of the fittest. In order to keep the best individuals, the fittest are copied to the next generation without any change. The genetic operation of crossover creates new individuals through the recombination of the genes from the previous generation. Two independent parents are selected based on the probability determined by the fitness. A mutation point in the string is chosen at random and the single character at that point is changed randomly. The changed individual is copied to the new

generation.

A set of strings is used to represent the population and each string is evaluated by the fitness function. Another generation is created according to the performances of individuals of the current generation. During the formation of the following generation, the genetic operators of reproduction, crossover and mutation are utilized.

The process of the evolutionary algorithm is outlined below: [29]

Input:$\mu, \lambda, \Theta_l, \Theta_r, \Theta_m, \Theta_s$

Output: a^*, the best individual found during the run, or

P^*, the best population found during the run.

1 $t \leftarrow 0$;

2 $P(t) \leftarrow$ initialize(μ);

3 $F(t) \leftarrow$evaluate($P(t), \mu$);

4 **while** ($l(P(t), \Theta_l)$) true **do**

5 $P'(t) \leftarrow$ recombine $(P(t), \Theta_r)$;

6 P"$(t) \leftarrow$ mutate $(P'(t), \Theta_m)$;

7 $F(t) \leftarrow$ evaluate $(P$"$(t), \lambda)$;

8 $P(t+1) \leftarrow$ select(P"$(t), F(t), \mu, \Theta_s$);

9 $t \leftarrow t+1$;

where μ and λ denote the parent and offspring population sizes. $P(t)$ characterizes a

population at generation t. Parameter sets Θ_r, Θ_m and Θ_s are used to represent the characteristics of recombination, mutation and selection.

7.2 The evolution of the walking algorithm

In the trajectory based gaits generation algorithm introduced in Chapter 5, there are various parameters to tune. Four of the parameters (θ_e, T_{vh}, T_{ss} and z_{fe}) which affect the performance greatly are optimized through EA. The walking performance is evaluated from the ZMP trajectory. The associated fitness function is:

$$F = \frac{1}{\sum_n^{i=1}((x_{zmp}(i) - x_{dzmp}(i))^2}$$

x_{dzmp} is the desired ZMP trajectory which is chosen to have the largest margin. The fitness function is the inverse of the variance between the real ZMP trajectory and the desired ZMP trajectory. This ensures that after the evolution, the real ZMP trajectory comes close to the desired ZMP trajectory.

Table 7.1 lists the parameters used in the evolutionary algorithm.

Table 7.1: Parameters for the evolutionary algorithm

Parent size μ	20
Offspring size λ	40
Generation	100
Crossover Ratio	0.7
Mutation Ratio	0.15
Reproduction Ratio	0.05

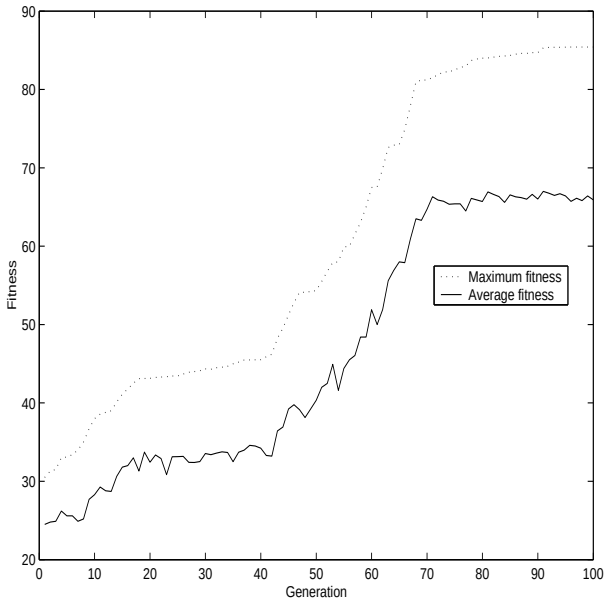

Figure 7.1: Fitness changing with generation

As shown in Figure 7.1, both the maximum fitness and average fitness converge after about 100 generation. In this evolutionary algorithm, the best individual in each generation is replicated to the next generation.

Table 7.2: Parameters of walking simulation

Parameter	value
step length	0.115 m
walking speed	0.1 m/sec

Figures 7.2 and 7.3 show respectively the ZMP trajectory before and after the evolution. Figure 7.4 shows the simulation of the biped robot climbing up stairs.

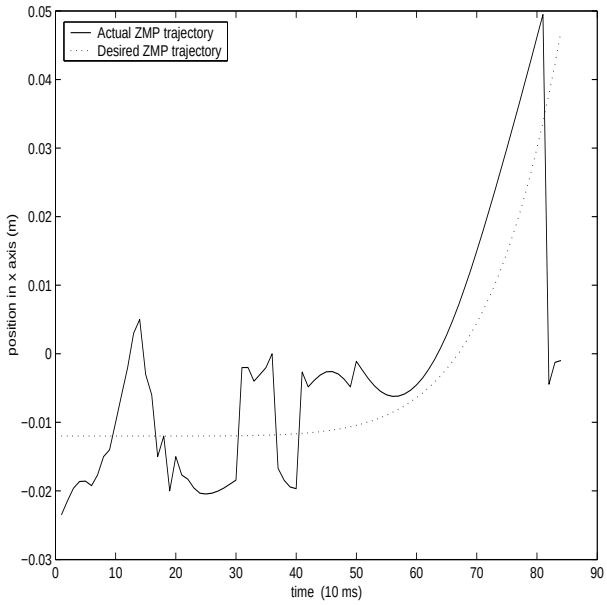

Figure 7.2: ZMP before evolution

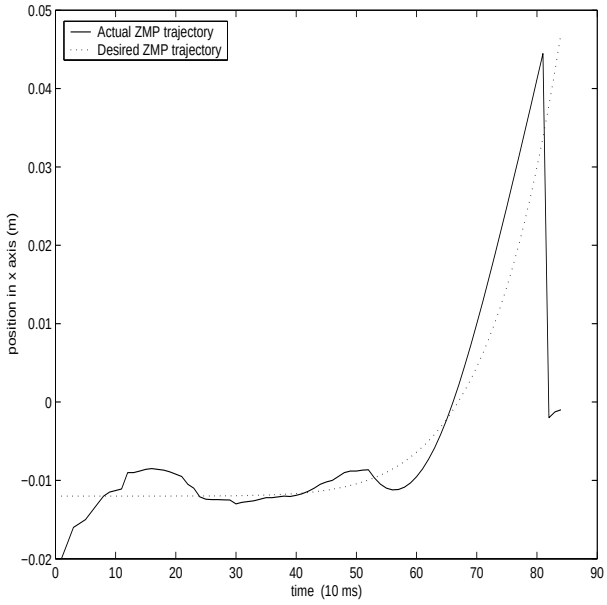

Figure 7.3: ZMP after evolution

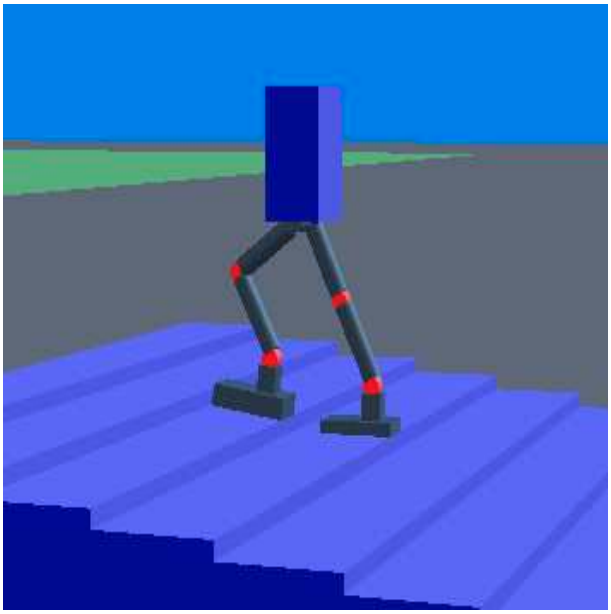

Figure 7.4: Simulation of climbing stairs

Chapter 8

Realized Functions and Algorithms

The robot successfully performed at the FIRA Robot World Cup 2003 and realized the following functions : (1) Robot Dash. (2) Obstacle Run. (3) Penalty Kick. (4) Goal Keeping.

8.1 Robot Dash

In the Hurosot (Humanoid robot soccer tournament) category of the FIRA competition, each biped robot is required to compete in 3 tasks. The first task is the Robot Dash, where the speed of the humanoids is the only criteria for comparing performance. The robot dash challenge is a sprint event for humanoid robots. Fast walking is very difficult to realize in biped robots, and Robosapien used a dynamic balance algorithm to improve the walking speed while maintaining a steady gait. In the competition, RoboSpien took 25 seconds to finish 1.2 meter walking. The runner up, in

comparison, took nearly thrice the time. (Figure 8.1)

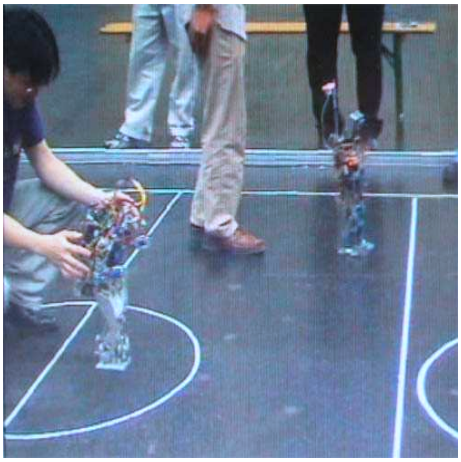

Figure 8.1: Robot dash

8.2 Penalty kick and goal keep

The second task is Penalty Kick and Goal Keep. In this challenge, the robot must approach and kick a ball positioned on the penalty marker into a goal. A robot from a different team will act as goal keeper during this task. The distance from the penalty marker to the goal is dependent on the robot height. This task requires that the robot use artificial intelligence techniques to locate the ball and the goalpost, and kick the ball with a best direction. Robosapien managed to score 5 goals in 6 tries: a very commendable performance even by human standards! (Figure 8.2)

Goal keep is a very difficult task. It requires the robot to locate the ball in a short time and, move quickly and stop the ball. Figure 8.3 shows that Robosapien is trying to stop a ball.

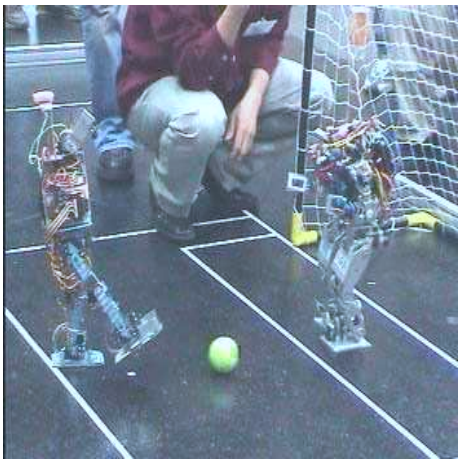

Figure 8.2: Penalty kick

8.3 Obstacle Run

In the third and the toughest of all tasks, the Obstacle Run, the robots have to overcome two challenges. The first is to walk along a path avoiding randomly placed obstacles in front of the robot. And secondly, in addition to avoiding the obstacles, the robots are also required to remember the paths they have taken. Robosapien used IR proximity sensors to detect the obstacles, with a servomotor driving the IR sensor to scan laterally, and a digital compass to sense the direction. The best record for RoboSapien in Obstacle Run is that it successfully accomplished the task in all the 5 rounds. Based on its performance in all three categories, the Robosapien brought home the overall trophy in the FIRA hurosot category [**?**]. (Figure 8.4)

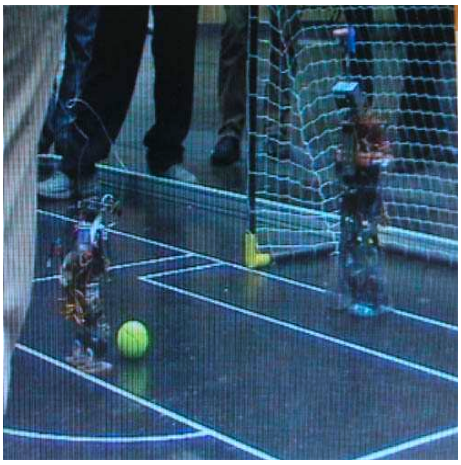

Figure 8.3: Goal keep

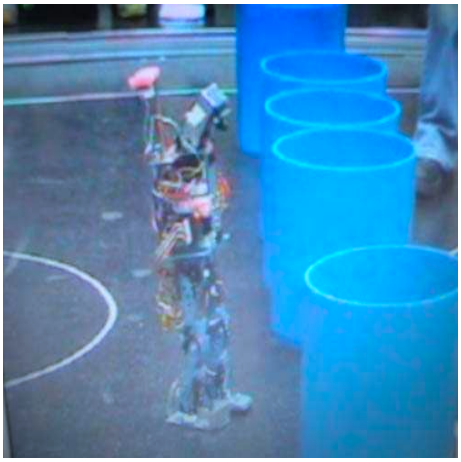

Figure 8.4: Obstacle run

Chapter 9

Conclusion

In recent years, dozens of biped robots have been developed and many researchers are working on biped walking algorithms. Great progress has been made in biped robot field while at the same time there are still many issues need to be studied and solved.

In this thesis, the background and relevant research on biped robot development and walking control are reviewed, a dynamic walking algorithm adapting to various terrains is synthesized and the development of a small size biped robot is presented.

A walking algorithm is synthesized and the simulation results are provided. The proposed walking algorithm can adapt to various terrains such as flat ground, rough terrain and stairs. Besides, the algorithm can enable the robot to start walking from any phase of the walking cycle.

The developed humanoid robot has 17 DOF and is equipped with various sensors: video camera, Infra-red sensor, digital compass, tilt sensor, force sensor. The robot has the ability to walk fast. It is able to detect and avoid obstacles. Besides, it is

able to do some complicated actions such as standing on one foot and kicking a ball.

The robot joined the FIRA World Cup 2003, Vienna and won first place in HuroSot (Humanoid robot soccer competition) category.

Bibliography

[1] T. McGeer, "Passive dynamic walking," *Int.J.Robot.Res.*, vol. 9, no. 2, pp. 62–82, 1990.

[2] S. Kajita, T. Yamaura, and A. Kobayashi, "Dynamic walking control of a biped robot along a potiential energy conserving orbit," *IEEE Trans. Robot. Automat.*, vol. 8, no. 4, 1992.

[3] Y. Zheng and J. Shen, "Gait synthesis for the sd-2 biped roobt to climb sloped surface," *IEEE Trans. Robot. Automat.*, vol. 6, no. 1, pp. 86–96, 1990.

[4] W. T. M. III, "Real-time neural network control of a biped walking robot," *IEEE Contr. Syst.*, vol. 14, pp. 41–48, 1994.

[5] C.-L. Shih, "Ascending and descending stairs for a biped robot," *IEEE Trans. Syst., Man, Cybern.*, vol. 29, no. 3, 1999.

[6] J. Pratt, C.-M. Chew, A. Torres, P. Dilworth, and G. Pratt, "Virtual model control: an intuitive approach for bipedal locomotion," *Int.J.Robot.Res.*, vol. 20, no. 2, pp. 129–143, 2001.

[7] K. Hirai, M. Hirose, Y. Haikawa, and T. Takenaka, "The development of honda humanoid robot," *Proc. IEEE Int. Conf. Robotics and Automation*, pp. 1321–1326, 1998.

[8] P. Sardain, M. Rostami, and G. Bessonnet, "An anthropomorphic biped robot: dynamic concepts and technological design," *IEEE Trans. Syst., Man, Cybern.*, vol. 28, no. 6, 1998.

[9] N. Kanehira, T. Kawasaki, S. Ohta, T. Isozumi, T. Kawada, F. Kanehiro, S. Kajita, and K. Kaneko, "Design and experiments of advanced leg module (hrp-2l) for humanoid robot (hrp-2) development," *Proc. 2002 IEEE-RSJ Int. Conf. Intelligent Robots Systems EPFL, Lausanne, Switzerland*, pp. 2455–2460, 2002.

[10] A. Konno, N. Kato, S. Shirata, and M. U. T. Furuta, "Development of a light-weight biped humanoid robot," *Proc. 2000 IEEE-RSJ Int. Conf. Intelligent Robots Systems*, pp. 1565–1570, 2000.

[11] C.-L. Shih, W. A. Gruver, and T.-T. Lee, "Inverse kinematics and inverse dynamics for control of a biped walking machine," *J. Robot. Syst.*, vol. 10, no. 4, pp. 531–555, 1993.

[12] J. E. Pratt and G. A. Pratt, "Exploiting natural dynamics in the control of a 3d bipedal walking simulation," *Int.Conf.on Climbing and Walking Robots, Portsmouth, UK, September*, 1999.

[13] J. H. Park, "Impedance control for biped robot locomotion," *IEEE Trans. Robot. Automat.*, vol. 17, no. 6, pp. 870–882, 2001.

[14] S. Kajita and K. Tani, "Experimental study of biped dynamic walking," *IEEE Contr. Syst.*, 1996.

[15] M. Vukobratovic and D. Juricic, "Contribution to the synthesis of biped gait," *IEEE Trans. Bio-Med. Eng.*, vol. BME-16, no. 1, pp. 1–6, 1969.

[16] A. Takanishi, M. Ishida, Y. Yamazaki, and I. Kato, "The realization of dynamic walking robot wl-10rd," *Proc. 1985 Int. Conf. Advanced Robotics*, pp. 459–466, 1985.

[17] Q. Huang, K. Yokoi, S. Kajita, K. Kaneko, H. Arai, N. Koyachi, and K. Tanie, "Planning walking patterns for a biped robot," *IEEE Trans. Robot. Automat.*, vol. 17, no. 3, 2001.

[18] J. Furusho and A. Sano, "Sensor-based control of a nine-link biped," *Int. J. Robot. Res.*, vol. 9, no. 2, pp. 83–98, 1990.

[19] T. A. McMahon, "Mechanics of locomotion," *Int.J.Robot.Res.*, vol. 3, no. 2, pp. 4–28, 1984.

[20] R. E. Goddard, Y. F. Zheng, and H. Hemami, "Control of the heel-off to toe-off motion of a dynmaic biped gait," *IEEE Trans. Syst., Man, Cybern.*, vol. 22, no. 1, 1992.

[21] Y. F. Zheng, "Acceleration compensation for biped robots to reject external disturbances," *IEEE Trans. Syst., Man, Cybern.*, vol. 19, no. 1, 1989.

[22] J. Yamaguchi, E. Soga, S. Inoue, and A. Takanishi, "Development of a biped robot-control method of whole body cooperative dynmaic biped walking," *Proc.*

1999 IEEE Int. Conf. Robotics and Automation, Detroit, Michigan, pp. 368–374, 1999.

[23] G. Taga, Y. Yamaguchi, and H.Shimizu, "Self-organized control of bipedal locomotion by neural oscillators in unpredictable environment," *Biol. Cybern.*, pp. 147–165, 1991.

[24] E. R. Westervelt, J. W. Grizzle, and C. C. de Wit, "Swiching and pi control of walking motions of plannar biped walkers," *IEEE Trans. Automat. Contr.*, vol. 48, no. 2, pp. 308–312, 2003.

[25] http://www.yobotics.com

[26] K. Hirai, "The honda humanoid robot," *Proc. 1997 IEEE-RSJ Int. Conf. Intelligent Robots Systems, Grenoble, France*, pp. 499–508, 1997.

[27] C.-L. Shih and C. J. Chiou, "The motion control of a statically stable biped robot on an uneven floor," *IEEE Trans. Syst., Man, Cybern.*, vol. 28, no. 2, 1999.

[28] http://www 2.cs.cmu.edu/cmucam/

[29] K. D. Jong, L. Fogel, and H.-P. Schwefel, *Handbook of Evolutionary Computation.* IOP Publishing Ltd and Oxford University Press, 1997.

[30] G. Wyeth, D. Kee, and T. F. Yik, "Evolving a locus based gait for a humanoid robot," *in Proc. IROS2003*, 2003.

[31] D. G. and H. Hu, "A hybrid evolutionary algorithm for gait generation of sony legged robots," *in Proc.* 28^th *Annual Conference of the IEEE Industrial Electronics Society, Sevilla, Spain*, 2002.

[32] http://www.fira.net

Author's Publications

1. An evolutionary algorithm for trajectory based gait generation of biped robot, R. Zhang, P. Vadakkepat and C.M. Chew, proceedings of the international conference on Computational Intelligence, Robotics and Autonomous Systems (CIRAS 2003), December 15-18, 2003, Singapore.

2. Motion Planning for biped robot climbing stairs, R. Zhang, P. Vadakkepat and C.M. Chew, Proceedings of FIRA Robot World Congress, October 1-3, 2003, Vienna, Austria.

3. Mechanical design and control system configuration of a humanoid robot, R. Zhang, P. Vadakkepat and C.M. Chew, proceedings of the international conference on Computational Intelligence, Robotics and Autonomous Systems (CIRAS 2003), December 15-18, 2003, Singapore.